

## Mineralogy of deep-sea sediments around Réunion Island (Western Indian Ocean)

AGATA DUCZMAL-CZERNIKIEWICZ<sup>1</sup>,  
STANISŁAW LORENC<sup>1</sup>, KARL STATTEGGER<sup>2</sup>

<sup>1</sup> Institute of Geology, Adam Mickiewicz University, Poznań

<sup>2</sup> Institute of Geological Science, Kiel University, Germany

**Abstract:** Detailed petrographic and mineralogical analyses were performed in order to determine and classify ocean sediments in the vicinity of Réunion Island. Surface sediments from the ocean floor and samples from cores of thickness down to 560 cm were classified as hemipelagic muds of volcanogenic origin, pelagic calcareous oozes and basaltic breccia. Heavy, light and pelitic fractions were investigated separately. Basaltic breccia consists of rock fragments and glass shards. Hemipelagic muds consist mostly of basaltic fragments, plagioclases, pyroxenes and olivines, basaltic glass shards, zeolites, and clay minerals. Moreover, various amounts of carbonate and siliceous bioclasts also occur. Pelagic oozes (nannoplankton and foraminifera) are composed mainly of carbonate bioclasts and micrite.

The mineral composition of the sediments and the relationship between pelagic and volcanogenic components were determined referring to the depth and distance from the Réunion Island. The sediments from the southernmost profile are different than others taken at a smaller distance from the island not only with respect to the fossil assemblage but also with respect to the occurrence of concretions (and quartz, staurolite and apatite) and greater degree of glass alteration. These sediments were formed under the conditions of pelagic sedimentation, and so the slow sedimentation rate facilitated the formation of concretions.

The mineral composition of the sediments differs according to the distance from the volcanic Réunion Island and the depth from which the sediment was sampled.

**Key words:** deep-sea sediments, mineralogy, Réunion Island.

### Introduction

Oceanological studies, including geological investigations, were initiated in the second part of the nineteenth century. The famous CHALLENGER

cruise in 1872–1876 was a particular example of these researches. Modern studies of ocean basins began during the International Geophysical Year (1957–1958), when twenty three research vessels explored the ocean bottom.

Since 1966, deep geological drillings have been carried out, first within the framework of DSDP project (GLOMAR CHALLENGER vessel), subsequently within the framework of ODP project (JOIDES RESOLUTION vessel). Other international projects have been also involved in the investigation of oceans and seas. One of them, financed by the German Ministry of Research and Technology, concerned within plate volcanic activity aspects, including hot-spots. During the SO87 cruise with RV SONNE in June 1993, the ocean bottom around volcanic Réunion Island was explored.

Volcanic rocks from Réunion Island have been investigated since 1960th (Upton & Wadsworth 1966; McDougall 1971; Tilley *et al.* 1971; Albarède & Tammagnan 1980; Gillot & Nativel 1982; Deniel *et al.* 1992). The island was formed as a result of the within plate volcanism – a product of the oceanic crust hot-spot system (Morgan 1981; Molnar & Stock 1987; Duncan *et al.* 1989). According to the model proposed by Duncan (1990), the relative movement of the hot-spot is from north-west to the present position, about 300 km away from the island. However, during the investigations carried out during the SO87 cruise, no traces of volcanism were found in the area indicated by Duncan (1990). Bathymetric data and determination of the rock age (Lénat *et al.* 1989; Fretzdorff 1997) confirmed a relatively young volcanism (5 million years) that initiated the formation of the island.

Philippot (1984) first investigated sediments around the island. He compared island sediments to the Quaternary marine sediments around the island, of volcanic origin. Pyroclastic sediments were identified, among them tuffs, lapilli and volcanic bombs (Upton & Wadsworth 1966; Philippot 1984), which originated as a result of the explosive activity of the island volcanoes. The deltas of many rivers, which cut the volcanic rocks with deep valleys, contain very young sands, silts and clays, in which smectites and kaolinite are the main clay components (Philippot 1984). Kolla & Biscaye (1973) and Kolla *et al.* (1976) described clay minerals in the sediments from Western Indian Ocean. They distinguished montmorillonite, illite, chlorite and kaolinite minerals in the bottom oceanic sediments.

The phillipsite–thomsonite–analcime group is the most frequent paragenesis occurring in hydrothermally altered rocks on Réunion Island (Philippot 1984). Zeolites are changed into clay minerals, mainly smectites, which are the main component of the sediments in the western part of the island. Smectites, enriched in magnesium and calcium, also fill the vesicles in weathered basalts (Philippot 1984). Minerals of the chlorite group were formed as a result of ignimbrites alteration, which occur in the northeastern part of *Piton des Neiges* (Rocher & Westercamp 1989).

This paper presents detailed mineralogical studies of the ocean bottom sediments. The authors distinguish detrital and autigenic components including

light, heavy and pelitic fraction of the sediments. Typical biogenic components were also examined and sediment age determination on the basis of nannoplankton was performed. The aim of this work was to find out relationship between authigenic and detritic components and the influence of volcanic activity on the mineralogical composition of the bottom sediments.

Volcanic rocks collected during the SO87 cruise were studied by Fretzdorff (1997). The sediments were described by Stattegger and Lorenc (Stoffers *et al.* 1994). This paper presents the results of petrological and mineralogical studies of sediments, performed by A. Duczmal-Czernikiewicz during her PhD-studies at the Institute of Geology, Adam Mickiewicz University, Poznań.

## Geological setting of Réunion

In the western part of the Indian Ocean, bordered by the eastern edge of the African continent, there are a few abyssal basins whose depths exceed 5 km. The largest of them are the Somali, Mascarene and Mauritius Basins. The Somali Basin is located in the north, and its maximum depth is 5437 m; Seychelles Islands separate it from Madagascar. The Mascarene Basin is filled with sediments, mainly carbonates, which build the Saya de Malha and Nezareth banks. The sediments are over 1600 m thick. Mauritius, Réunion and Rodriguez (the Mascarene Islands) are located in the southern part of the basin, where the greatest depths reach 5432 m (Fig. 1). The Mauritius Basin, bordered by Madagascar in the west, reaches a depth of 5815 m. Its bottom is made of basaltic rocks, cut with deep fractures of the oceanic crust.

Réunion lies in the western part of the Indian Ocean (55°32' E and 21°07' S), about 700 km east of Madagascar, about 1200 west of the mid-Indian ridge with the Mauritius Fracture Zone and Wilshaw Fracture Zone to the east and to the west, respectively.

Réunion is elliptical in shape (50 x 70 km), with the longer axis in the NW-SE direction. It occupies an area of 2512 km<sup>2</sup> and reaches over 7000 m above the ocean bottom. Réunion is formed by two volcanic cones: *Piton des Neiges* in the north-western part, with a height of 3069 above sea level, and *Piton de la Furnaise* in the south-western part, 2631 m above sea level. At the base, at the depth of 4000 m below sea level, the entire volcanic complex has a diameter of about 190 km. The average slope of the submarine volcanoes at this depth is 4,5° (Upton & Wadsworth 1965).

### Piton des Neiges

*Piton des Neiges* is an extinct shield volcano with a diameter of approximately 50 km at the base. Two basic stages leading to the cone formation

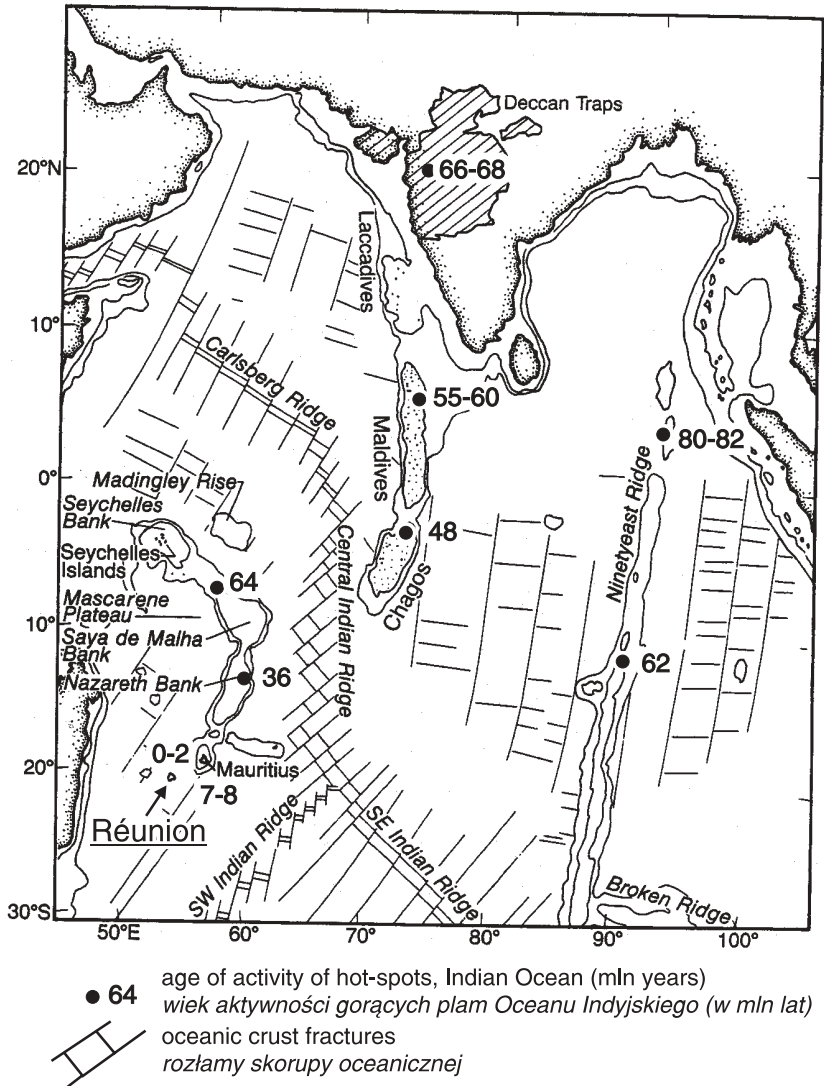


Fig. 1. Location of Réunion hot-spot and major structural features of the Western Indian Ocean (after Duncan *et al.* 1989).

Położenie gorącej plamy Réunion oraz główne cechy strukturalne Zachodniego Oceanu Indyjskiego (wg Duncan i in. 1989).

have been distinguished (Upton & Wadsworth 1966, 1972 a, b; McDougall 1971; Gillot & Nativel 1989; Deniel *et al.* 1992):

1. Shield Building stage, directly connected with the oceanite series. Two series were identified in this stage:

- Older Oceanite<sup>1</sup> Series: < 2 million years, composed of pyroclastic breccia and brecciated flows of basalt lavas, cut with syenite intrusions,
- Younger Oceanite Series, from approximately 2 million years to 430 000 years BP. The flows of olivine basalts and oceanites of the normative olivine-hypersthene type, which are alkaline and tholeiite basalts formed the Younger Oceanite Series.

2. Post Shield Building stage, forming differentiated series, represented by lava flows composed of hawaite and benmoreite basalts and Q-normative benmoreites and trachytes. The volcanic activity of this stage occurred 290 000–12 000 years ago.

Fretzdorff (1997) compared the age and geochemical variability of the island rocks with their marine counterparts and determined that the explosive activity of *Piton des Neiges* occurred from 260 000 to 30 000 years ago. Pyroclastic rocks found on the island were dated by K-Ar and Th-U methods (Gillot & Nativel, 1982; Deniel *et al.*, 1992), whereas the age of their marine counterparts was determined using oxygen isotopes in *Globigerinoides ruber* planktonic foraminifera (Fretzdorff 1997).

### **Piton de la Furnaise**

Active for 530 000 years, *Piton de la Furnaise*, a shield volcano, occupies the southeastern part of the island. Contemporary lava outflows and seismic activity occur on average every 14 months (Nercessian *et al.* 1996; Sapin *et al.* 1996). Presently, the volcano is in the early shield phase. It is mainly built of basaltic and oceanite lavas, geochemically similar to the oceanite series lavas of *Piton des Neiges*. The volcano cone forms U-shaped caldera, open to the east, thus facilitating the migration of lavas and volcanoclastic sediments to the ocean floor (Gillot *et al.* 1994). Slides of enormous lava flows lead to the formation of underwater avalanches and turbidites on the eastern side of Réunion (Ollier *et al.* 1998).

The investigation of sediments around the island conducted by Fretzdorff (1997) revealed that only one of the homogeneous marine tephra layer, composed of basalt, comes from *Piton de la Furnaise* and was dated of 67 000 years old. The other ash layers correspond to the pyroclastic rocks of *Piton des Neiges*.

### **Age of sediments around Réunion**

Present day foraminifera have been extensively investigated (Backman & Duncan 1988), the focus being on the determination of the sediment age

---

<sup>1</sup> The “oceanite” term was introduced by Lacroix to describe the picritic basalts of Réunion, containing over 40% of olivines (Lacroix 1936, cf. Albarède and Tamagnan 1982).

by means of  $^{14}\text{C}$  and  $^{18}\text{O}$  of foraminifera tests (Berger 1981; Duplessy *et al.* 1981; Bassinot *et al.* 1994). The sediments from the vicinity of Réunion are not older than 260 000 years (Fretzdorff 1997).

## Sample preparation and investigation methods

During the SO87 cruise samples were taken by three methods:

- redge samples, designated as DS, were taken from the bottom of the ocean,
- box samples, designated as GKG, were taken from the bottom surface up to the depth of 40 cm,
- core samples, designated as SL, were taken from gravitational cores, up to 5.60 m long, near the places from which box samples were taken.

The samples selected for mineralogical studies, are listed in Appendix 1 and located on the map in Fig. 2.

The pattern of investigations is presented in Fig. 3. At the first stage the sediments were described macroscopically; the descriptions made during the cruise (Stattegger & Lorenc, in: Stoffers *et al.* 1994) were incorporated. Smear slides were used for the microscopic observations (Rothwell 1987).

The sediments were then sieved, washed and separated into two fractions: above 0.063 and below 0.063 mm. In the subsequent investigations the non-separated sediment and the separated fractions were analysed.

## Grain size analysis

The sediments grain size was investigated by two methods: sieve analysis of the sand fraction, and laser analysis of the fines ( $< 0.063$  mm), and the bulk sediment (19 samples). Results of granulometric analyses are given in tables in Duczmal-Czernikiewicz 1999.

## Heavy mineral analysis

Twenty samples of the  $0.071 < \phi < 0.1$  mm and  $\phi < 0.063$  mm fractions were selected for the separation of heavy minerals. The powder of sodium polytungstate was dissolved in distilled water, and a heavy liquid with specific density of  $2.86 \text{ g/cm}^3$  was obtained. Heavy minerals were separated at the laboratory of the Institute of Geology, Adam Mickiewicz University. Thin sections were made from the heavy mineral fraction at the Institute of Geological Sciences, Polish Academy of Sciences in Cracow.

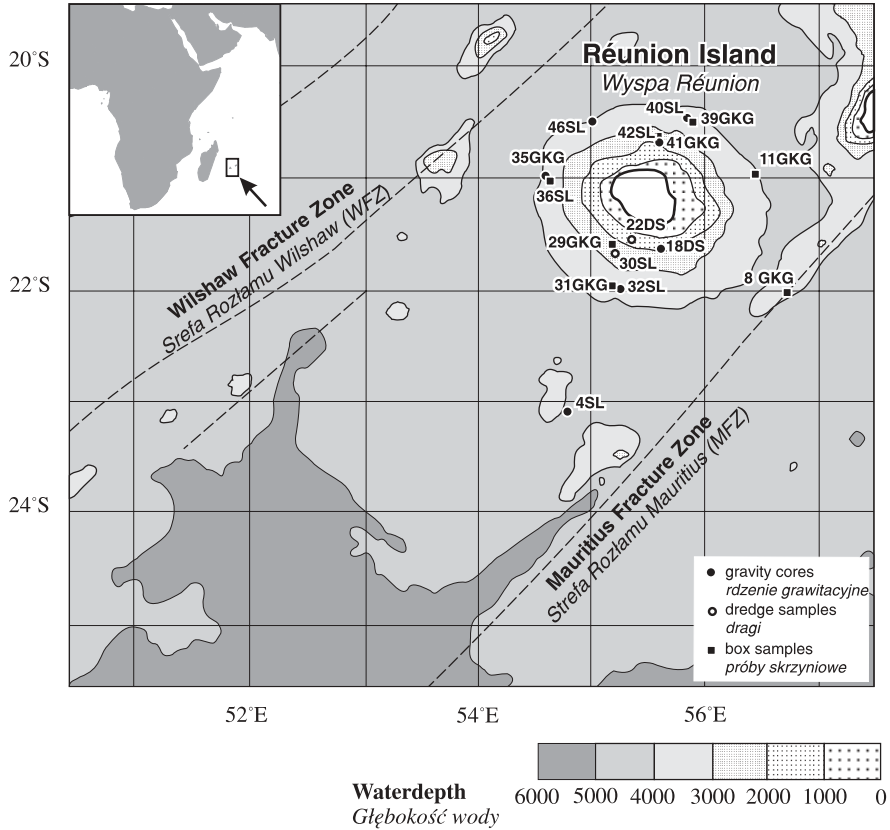


**Fig. 2.** Bathymetric map of the studied area and location of the stations (after Stoffers *et al.* 1994).

Mapa batymetryczna badanego obszaru i położenie miejsc pobrania próbek (wg Stoffersa i in. 1994).

### Scanning electron microscopy (SEM)

Observations under the scanning microscope were supplemented with a qualitative analysis of the chemical composition. SEM Hitachi S-530 microscope and EDX KEVEX micro-X 7000 spectrometer were used, at 25 kV and 100 nA. The analysis was made at the Institute of Mineralogy, Hannover University. The entire sediments and selected fractions were observed.

### Electron microprobe (EMP)

The sediment components of 30 samples (light and heavy fractions) were analysed with electron microprobe. The investigations were made at the In-

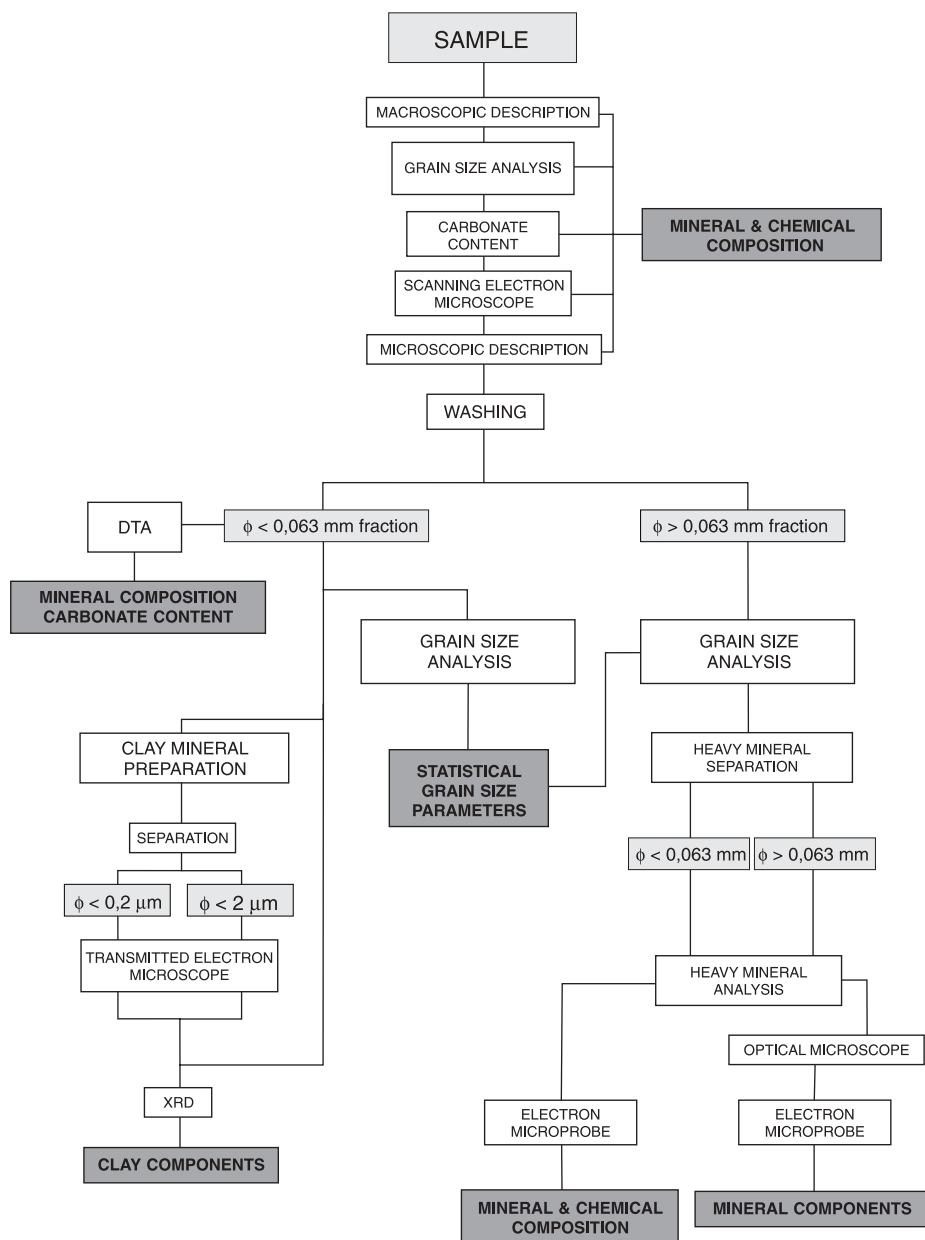


**Fig. 3.** Scheme of sample preparation and investigation methods.

Schemat preparatyki próbek i stosowanych metod badań.

stitute of Mineralogy, Hannover University and at the Institute of Geological Sciences at Wrocław University. In Hannover University, Cameca Camebax microprobe was used (15 kV and 18 nA). In the case of crystalline phases the co-

unting time was 10 s for each element and 5 s for the substrate. In the case of glass measurements, the time for K and Na was 2 s, whereas for other elements it was 5 s. In Wrocław, Cambridge Microscan M9 electron microprobe was used, under the following conditions: accelerating voltage 15 kV, beam current 5 nA, counting time 20 s.

## X-ray diffraction

X-ray analyses were made by the diffractometric method at the Institute of Geology, Adam Mickiewicz University, on URD-6 spectrometer, using Co and Cu lamps, Ni and Fe filters. Dry samples were analysed in the range of  $2-75^\circ 2\theta$ . Fractions  $< 2 \mu\text{m}$  ( $2-75^\circ 2\theta$  and  $59-64^\circ 2\theta$ ) and  $< 0.2 \mu\text{m}$  ( $2-40^\circ 2\theta$ ) were also investigated in order to determine the clay mineral phases. Organic substance, carbonate and Fe compounds were removed from the dry samples according to the sample preparation technique proposed by Jackson (1975) and modified by Moore & Reynolds (1998). The samples were saturated with Na ions in order to stabilize the basic peak of smectites in the  $14.5 \text{ \AA}$  range. Next, by means of a centrifuge the material was separated into fractions. Random samples were made from the  $< 2 \mu\text{m}$  fraction, and oriented samples, glycolated and heated at the temperature of  $550 \text{ C}$ , were made from the  $< 0.2 \mu\text{m}$  fraction. The selected diffractograms are presented in Figs. 12–16.

## Results

### Petrographic diversity

On the basis of petrographic investigations of 150 samples taken from the ocean bottom and the sediment cores (Fig. 4), the following lithologies were identified around Réunion: hemipelagic volcanogenic muds, pelagic carbonate oozes (nannoplankton and foraminifera) and sediment of volcanogenic basaltic breccia. Hemipelagic muds are the majority of the sediments around the island, whereas pelagic oozes occur of the southernmost profile, i.e. 4SL (Fig. 2). The basaltic breccia occurs on the eastern slope of *Piton de la Fournaise*.

Volcanogenic muds consist mainly of fragments of basaltic rocks, minerals of volcanic origin (plagioclases, pyroxenes and olivines), volcanic glass shards, zeolites and clay minerals. Moreover, there are different quantities of carbonate bioclasts and small quantities of siliceous ones. Pelagic oozes are mainly formed of carbonate bioclasts and micrite (Fig. 5). Fragments of basalt rocks and volcanic glass shards form the basaltic breccia.

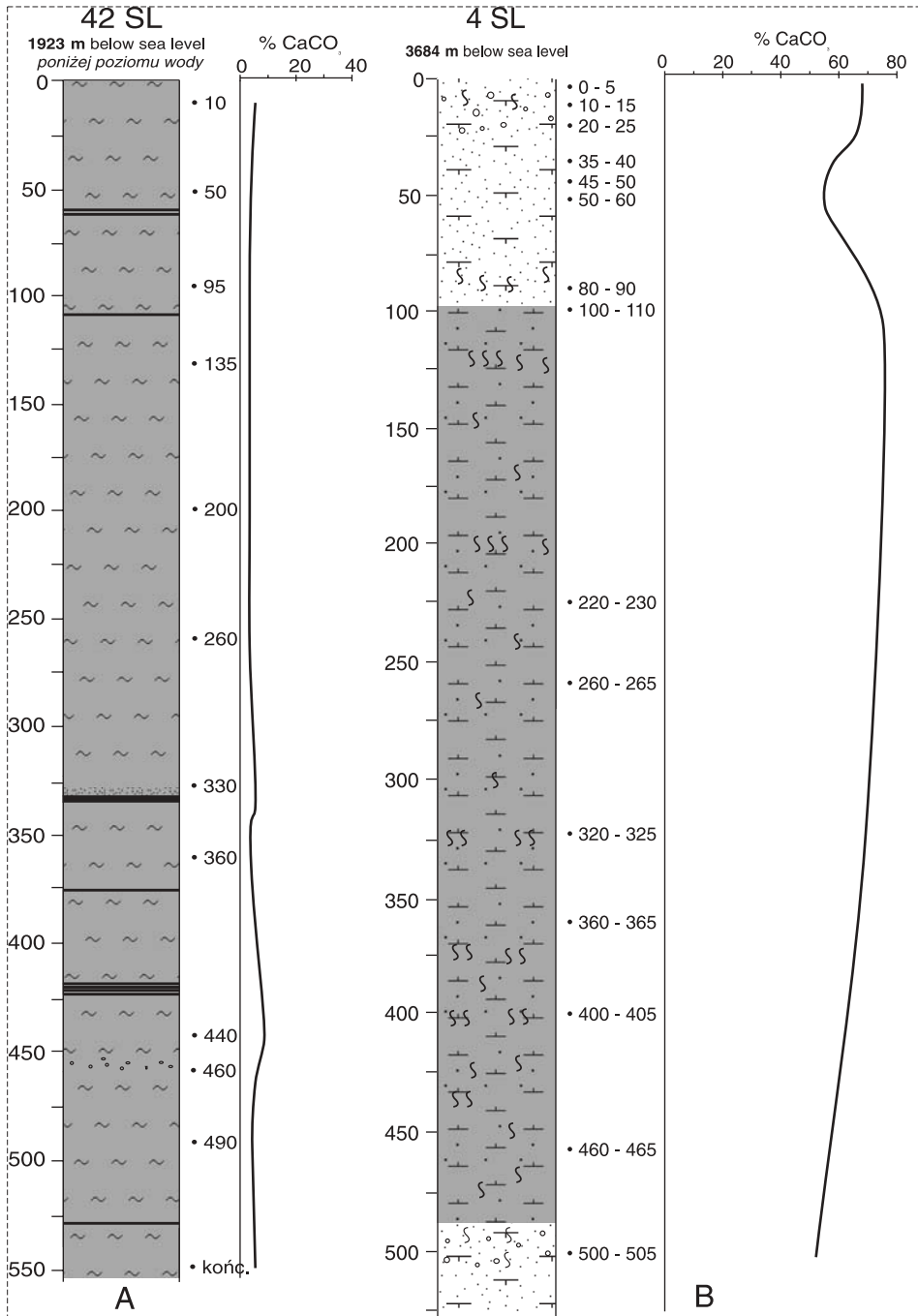


**Fig. 4.** Lithologic profiles of cores (after Stattegger and Lorenc, in: Stoffers *et al.* 1994).

Profile litologiczne rdzeni (wg Statteggera i Lorenca, w: Stoffers i in. 1994).



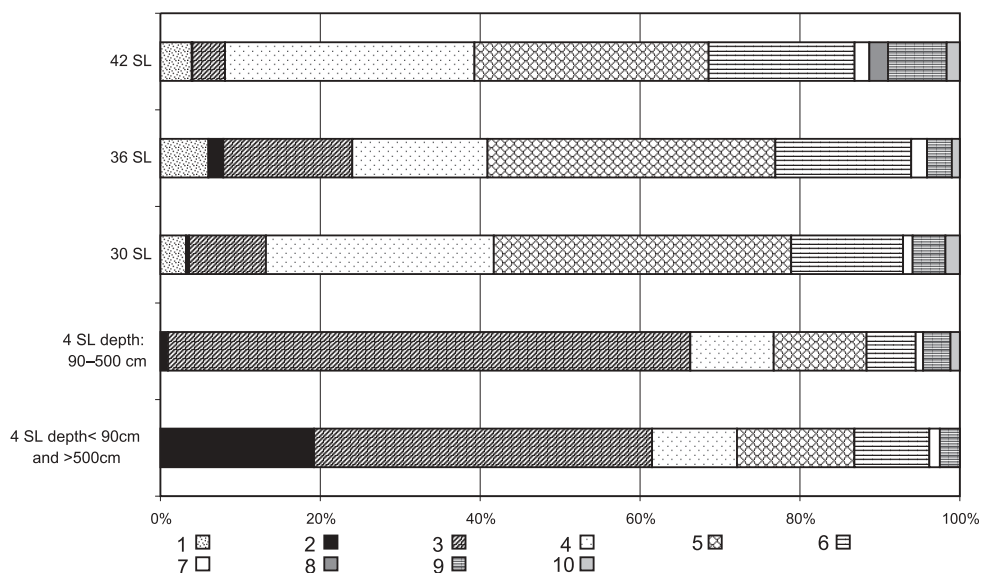


**Fig. 5.** Mineral composition of investigated sediments.

Skład mineralny badanych osadów.

1 – sil biocl (bioklasty krzemionkowe); 2 – foram (otwornice); 3 –  $\text{CaCO}_3$ ; 4 – lit clasts (litoklasty); 5 – plag (plagioklasy); 6 – ol + cpx (oliwiny + klinopiroksemy); 7 – glass (szkliwo wulkaniczne); 8 – pumice (pumeks); 9 – clay min (minerały ilaste); 10 – zeolites (zeolity)

## Light fraction components

The light fraction includes mainly bioclasts, feldspars and zeolites, and, in smaller quantities, crystals of carbonates and sediment rock fragments. Other components (muscovite, quartz) are rare.

## Bioclasts

The bioclasts include carbonate components, i.e. foraminifera and nannoplankton and siliceous fossils. Fish teeth are also common, whereas ostracods are very rare.

## Foraminifera

Planktonic foraminifera are the most common carbonate bioclasts. The dominant families include Globigerinidae (Globigerinoides) *Globigerina*

rubber, (Orbulininae) *Orbulina* sp. (Pl. 1, Fig. 1) and (Globorotarioidea) *Globorotalia truncatulinoides*. Equally frequent are (Diskorbinae) *Planodiscorbis rarscens*. Less common are foraminifera with trochospiral tests featuring point ornamentations or foraminifera with biserial tests (*Karreriella apiculari*). Benthic foraminifera with uniserial ribbed tests occur in small quantities. In surface sediments of the 22DS and 36SL sections there are foraminifera with agglutinated, planispiral tests (*Helenina anderseni*) as well as with elongated, cylindrical tests (*Protobotellina* sp.).

In the deeper parts of the 4SL section, at the depth of 80 cm below the bottom (3764 m below water surface), the number of foraminifera is decreasing, and they are etched and crushed.

## Nannoplankton

The other bioclasts are calcareous nannoplankton. They include species: *Gephyrocapsa oceanica* and *Emiliania huxleyi* (Pl. 1, Fig. 2) and discoasters. Six-arm or, less frequently, five-arm discoasters, *Discoaster brouweri*, with long straight arms (Pl. 1, Fig. 3). Five-arm discoasters are also represented by *Discoaster asymmetricus* (NN 11-NN 18) (asymmetric) and *Discoaster quinqueramus* (symmetric, bent arms) (NN 11). *D. triradiatus*, *D. petaliformis* with bifurcations at arm ends (NN 4-NN 5) and *D. quinqueramus* (NN 11) are also observed.

Coccoliths are present in all the sediments analysed, whereas discoasters are the main component of the nannoplankton oozes in the bottom part of the 4SL profile (below 100 cm).

Small aragonite needles with straight light extinction, (2–10  $\mu\text{m}$ ) are also present.

## Siliceous bioclasts

Sponge spicules are most frequent among siliceous bioclasts. Single spicules, always with a small channel inside, are most frequently seen in studied sediments (Pl. 1, Fig. 6). Triaxons and tetraxons were also recognized under binoculars and scanning microscope (Pl. 1, Fig. 4). A greater accumulation of skeletal elements of sponges is found in the samples in which carbonate bioclasts are in majority (e.g. 36SL 105). In profile 42SL sponge spicules constitute a considerable part of the sediment (Fig. 5). The sponge spicules in the lower parts of the profiles are highly fragmented; locally they serve as building material of the tests of agglutinated foraminifera (Pl. 1, Fig. 5). Radiolarians were found in all the sediments, although they are very rare.

It was confirmed by the XRD method that carbonate bioclasts are built of calcite. Microprobe analysis revealed low-magnesium calcite, like in other oceanic regions of the world (e.g. Seibold & Berger 1996).

**Plate 1.** SEM microphotographs of calcareous and silica bioclasts in selected samples.

Obrazy w mikroskopie skaningowym bioklastów węglanowych i krzemionkowych w wybranych próbkach.

**1.** *Orbulina* sp. 22 DS.

*Orbulina* sp. 22 DS.

**2.** *Emiliana huxleyi*, 22 DS.

*Emiliana huxleyi*, 22 DS.

**3.** *Discoaster brouweri* (Db), *Discoaster quinqueramus* (Dq), 4SL.

*Discoaster brouweri* (Db), *Discoaster quinqueramus* (Dq), 4SL.

**4.** Spongae spicule, triacsone, 36SL.

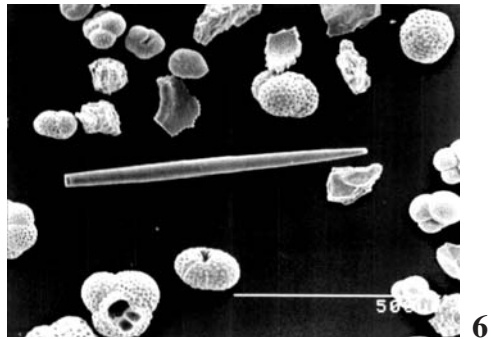
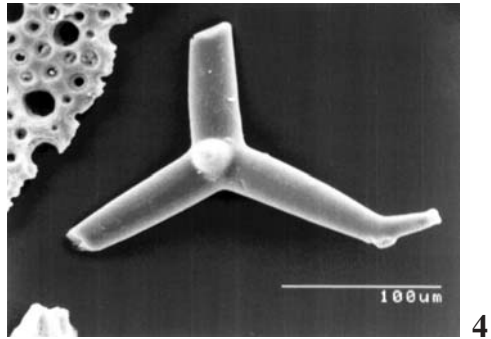
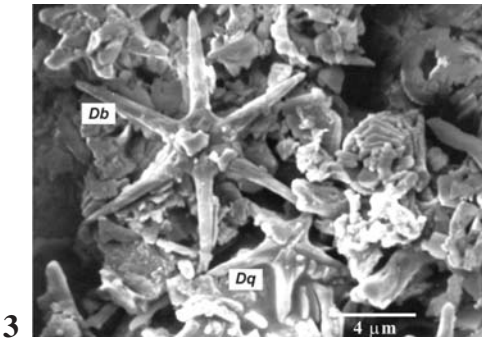
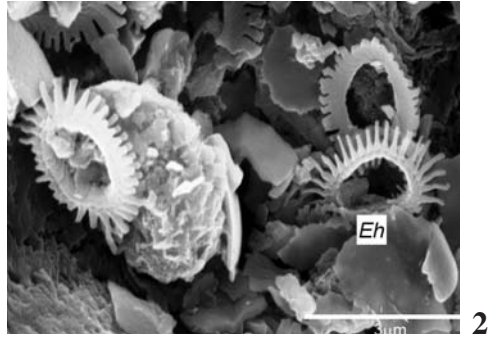
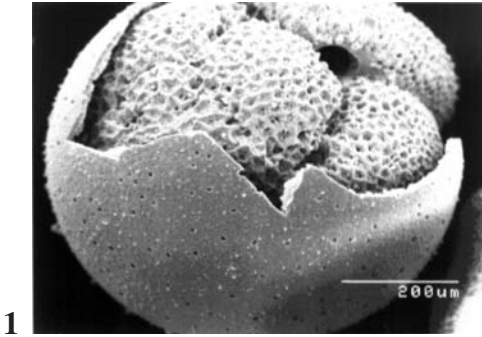
Igła gąbki, triakson, 36SL.

**5.** Agglutinated foraminifera, 22DS.

Otwornica aglutynująca, 22DS.

**6.** Single spongae spicule, 36SL.

Pojedyncza igła gąbki, 36SL.



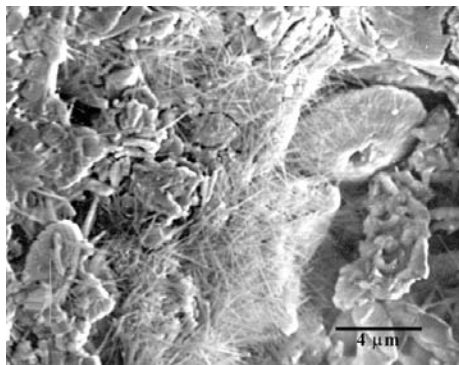


**Fig. 6.** SEM microphotograph of zeolites forming sphaerolites, 4 SL.  
Obraz w mikroskopie skaningowym zeolitów tworzących sferolity, 4SL.

## Zeolites

Because of the very small size of zeolites (a few microns) and considerable dispersion in the sediment, identification of these minerals by the optical method was very difficult. Zeolites were seen in some smear slides and under the electron scanning and transmitted microscope (Fig. 6). They form transparent, colourless crystals, elongated towards crystallographic axis Z, with a fairly distinct negative relief. Zeolite clusters in the form of sheaf-like crystal groups and sphaerolites were observed under the scanning microscope. The shape of the crystals and their optical features (light extinction at the angle of several degrees) helped to determine phillipsite.

## Feldspars, quartz and muscovite

Feldspars occur in the sediments forming crystals from a few microns to 1 cm; most often they are a few millimetres in size. Plagioclases are the main mineral components of the sediments in the upper part of the 36SL and the 30SL sections. They often contain inclusions of opaque minerals and, consequently, they occur in the heavy fraction of the sediment.

The chemical composition of matrix plagioclases from the basaltic rock fragments was studied by the electron microprobe method. The content of anortite varied from 82 to 67% (App. 3). The content of  $K_2O$  is small, corresponding to 0.39–0.94% of normative orthoclase. On the classification triangle (Fig. 7a) projection points lie in the labradorite-bytownite field. In the samples from the 32SL profile from the depths of 36 m and 46 m, as well as in the box samples (e.g. 35GKG), a lower content of  $Na_2O$  and  $CaO$  was observed.

Authigenic, automorphic quartz, was found very sporadically. Detrital quartz occurs in the  $>0.063$  mm fraction as fairly large grains. Muscovite flakes occur in the sediment very rarely.

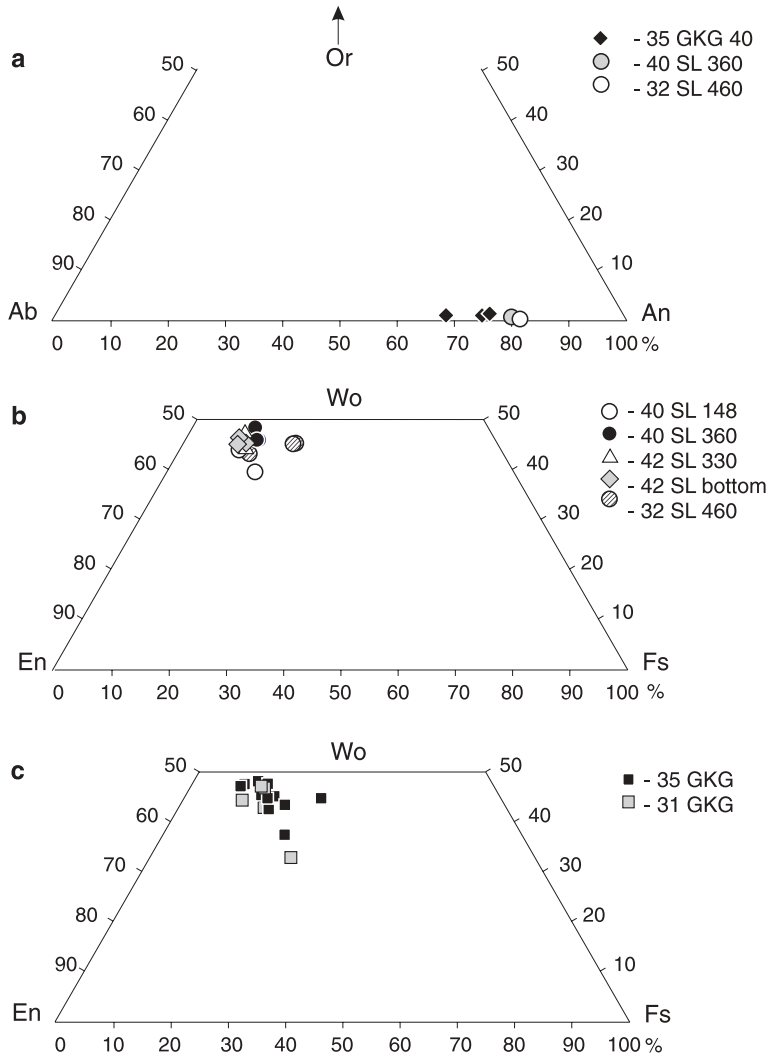


**Fig. 7a.** Composition of feldspars from box and core samples in Or-Ab-An triangle. Or – orthoclase, Ab – albite, An – anortite.

Skład chemiczny skaleni z próbek skrzyniowych i rdzeniowych na trójkącie Or-Ab-An. Or – ortoklaz, Ab – albit, An – anortyt.

**Fig. 7b–c.** Composition of clinopyroxenes from core and box samples, respectively. Wo-wollastonite En – enstatite Fs – ferrosilite.

Skład chemiczny klinopiroksenów, odpowiednio z próbek skrzyniowych i rdzeniowych, Wo – wollastonit, En – enstatyt, Fs – ferrosilit.

## Heavy fraction components

Heavy fraction usually constitutes from a few to several percent of the sample. In a few samples (8GKG, 11GKG, 18DS, 4SL 500–505, 40SL 460), heavy fraction constitutes 20–60% by weight.

The content of heavy fraction in the investigated grain fractions is shown in the charts (Figs. 8a and 8b). In the heavy fraction, lithoclasts are in majority. These components, together with opaque minerals, constitute 55–70% of the heavy fraction. Broken up basalts, highly mineralised, are dominant among the rock fragments. Opaque minerals constitute 1–2% of the studied fraction (exceptionally 5–11% of the sample by weight).

## Transparent minerals

Clinopyroxenes and olivines are dominant among transparent minerals (Fig. 9). The content of clinopyroxene is twice to four times greater than that of olivine. The remaining transparent grains are fragments of volcanic glass, plagioclases with ore inclusions, orthopyroxenes (42SL), amphiboles (42SL), rutile (4SL, 42SL), epidote, staurolite (4SL), mineralised bioclasts (mainly foraminifera), carbonate clasts and, very sporadically, biotite (8GKG 30–35).

## Clinopyroxenes

The content of clinopyroxene varies from 8 to over 30% of the heavy fraction (Fig. 9). The grains are usually greenish, in places colourless. In the 8GKG samples half of the pyroxene grains were light brown, mainly due to a higher content of titanium than in the green variety. In the coarser grain fractions, pyroxenes are elongated along crystallographic Z axis. However, most of the grains in the heavy fraction are crushed and irregular (Pl. 2, Fig. 1). Hour-glass-like pyroxenes are very sporadic (42SL 460).

Clinopyroxenes often contain inclusions of opaque minerals, usually chromite, magnetite and ilmenite. On the cleavage surface black and dark brown secondary compounds of Fe oxides and hydroxides can be observed, being the result of ore oxidation. Clinopyroxenes often occur as intergrowths with plagioclases or as a matrix of basaltic rocks.

Analysed with a microprobe, clinopyroxenes reveal a chemical content of enstatite – 37–47% by weight, wollastonite – 32–47% by weight, ferrosilite – 10–18% by weight (App. 2). The projection points on the classification triangle, both for box samples and core samples, are in the field of augite, and partly in the fields of diopside and salite (Figs. 7b and 7c). The analysed grains usually reveal zoning. In the border parts the content of Fe<sup>2+</sup> increases at the expense of

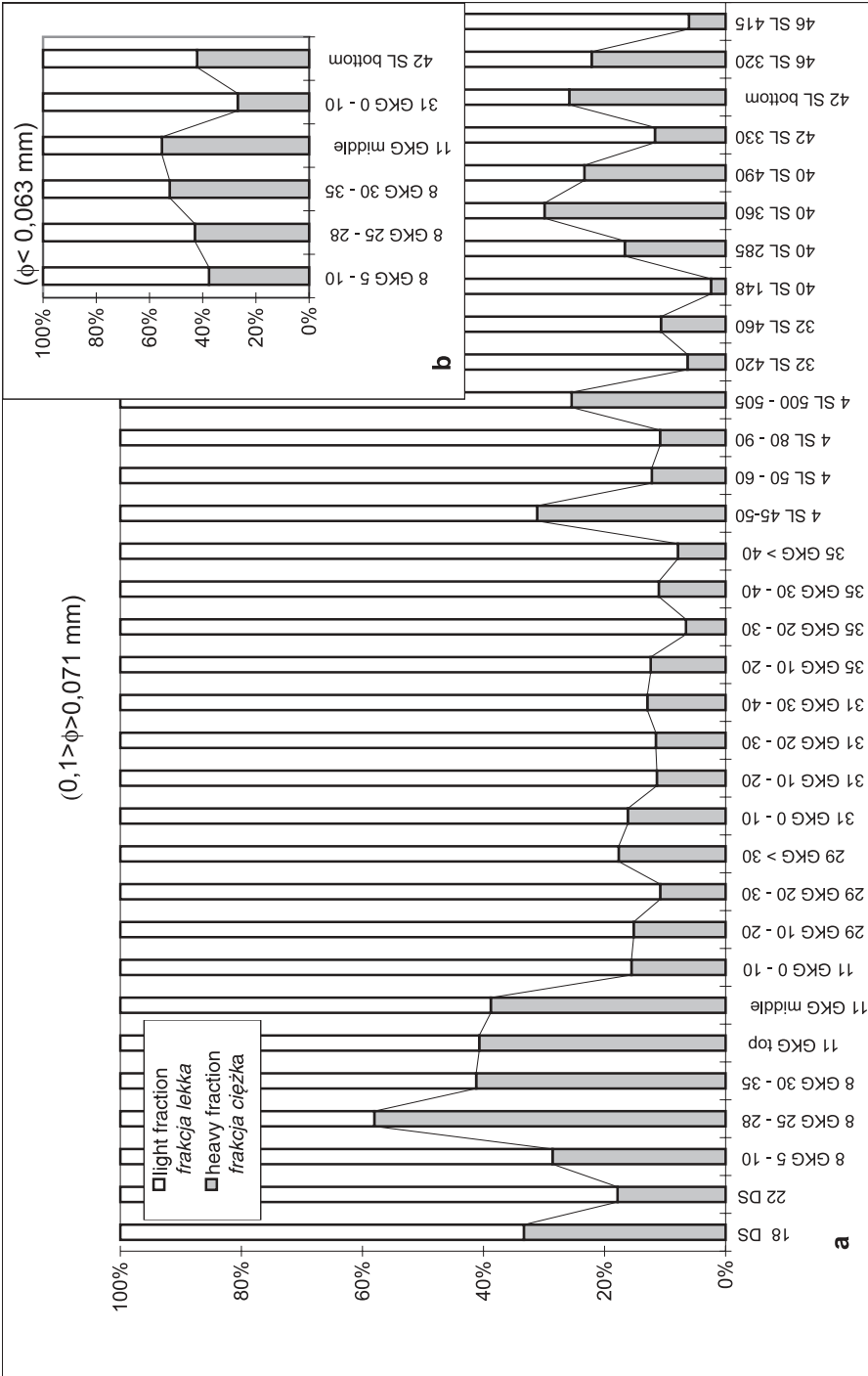


**Fig. 8.** Heavy fraction composition **a.** in  $0,071 < \phi < 0,1$  mm fraction. **b.** in  $\phi < 0,063$  mm fraction. Zawartość frakcji ciężkiej **a.** we frakcji  $0,071 < \phi < 0,1$  mm. **b.** we frakcji  $\phi < 0,063$  mm.

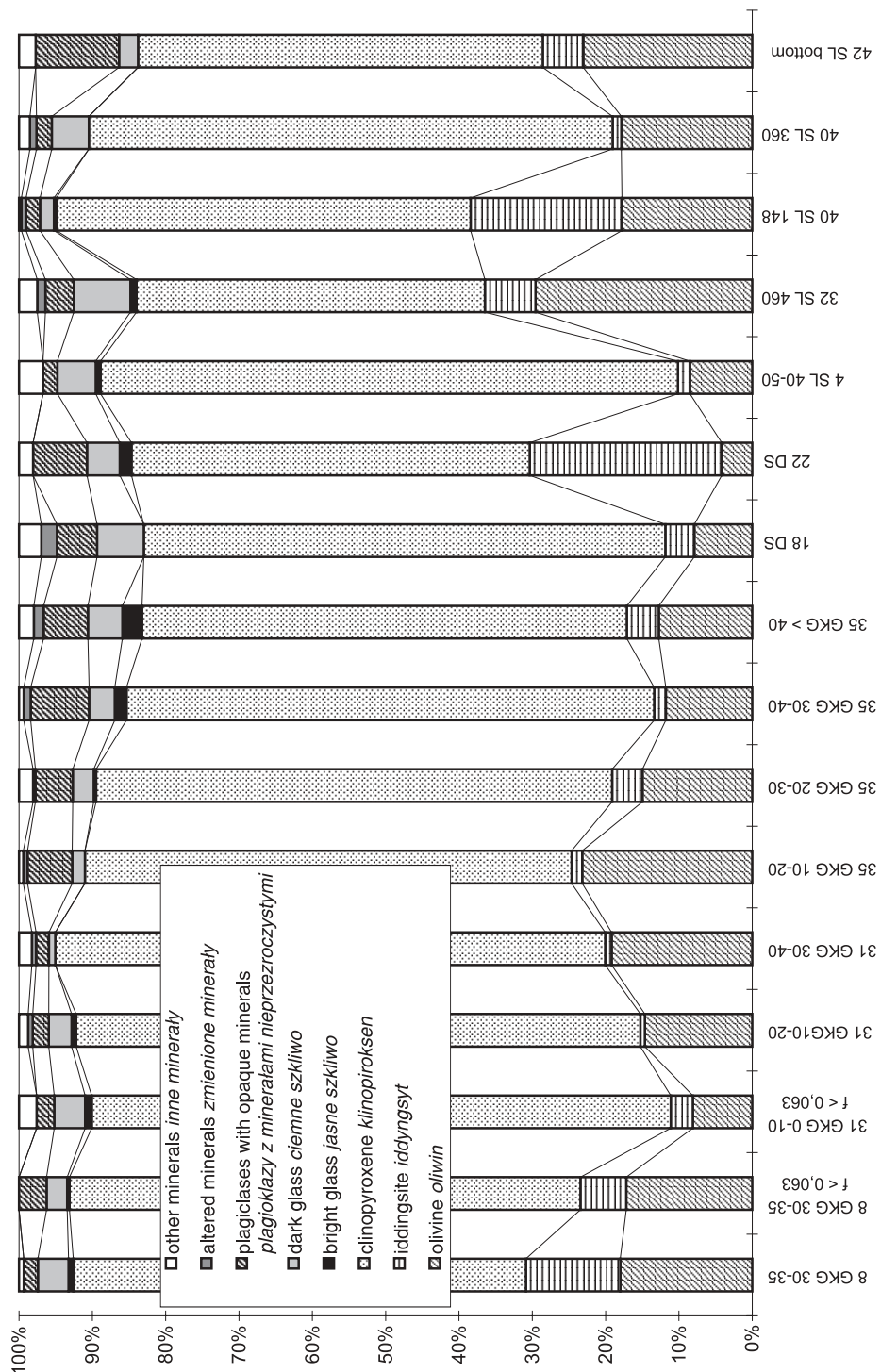


**Fig. 9.** Transparent mineral composition in fraction  $0,071 < \phi < 0,1 \text{ mm}$ .  
Zawartość składników przezroczystych we frakcji  $0,071 < \phi < 0,1 \text{ mm}$ .

Mg<sup>2+</sup>. In the grain centre the content of ferrosilite is 10–14% by weight, and increases to 24% at the borders. The increase of Mg<sup>2+</sup> content towards the edges of the grain is sporadically observed (En increases from 40–50%, 31GKG 10–20). In the samples from the deepest parts of the cores a low content of Fe is observed (Fs below 10% by weight).

## Olivines

The grains of unaltered olivines are sporadically encountered among heavy minerals (Fig. 9). Clean, automorphic crystals occur more frequently in the coarser grain fractions (> 0.25 mm). Olivines with inclusions of spinel and altered olivines, e.g. iddingsites (Pl. 3, Fig. 2), constitute a few percent of the heavy fraction. Olivines transformed into bowlingite are also present, particularly in the 4SL profile.

Olivine grains are colourless, sporadically lemon coloured. They usually occur in the sharp edged, isometric form, however rounded grains have also been observed. In profile 4SL kelyphite rims around olivines also occurred.

Chemical analyses revealed forsterite-rich composition of olivines. On average, there is 71–80% by weight of forsterite; consequently, these minerals are chrysolites. In some of the 35GKG and 31GKG samples and in the 40SL profile the content of the forsterite does not exceed 70% by weight. In some surface sediments, mainly from the area located east and south-west of the island, there are hialosiderites. In the samples from the northern and north-eastern part of the area the content of forsterite reaches 84–86% by weight. In most cases olivine grains are homogeneous with respect to their chemical composition. However, in some grains (35GKG > 40) the content of forsterite increases from 79 to 84% towards the grain edges.

The sediments from the profiles located near the island (46SL, 32SL 460) are much richer in olivine, and consequently the clinopiroxene/olivine ratio is nearly 1:1. They originated from the rocks corresponding to olivine basalts.

## Volcanic glass

Volcanic glass constitutes from less than 1% to nearly 3% by weight of the heavy fraction. In the studied profiles, at certain depths, e.g. 4SL 40–50, 4SL 80–90, 4SL 500–505, 32SL 320, an increased number of glass shards is observed. On average the sediment is then coarser grained and its components reveal a higher degree of alteration. These sediments can be correlated with the marine layers of volcanic ashes, identified by Fretzdorff (1997).

In the volcanic breccia from samples 11GKG, originating from the eastern part of the island, small particles with an openwork structure, characterized by the occurrence of many vesicles, are very frequent (Pl. 2, Fig. 2a). Glass also occurs

**Plansza 2**

**1.** Brown and bright grains of volcanic glass shards, op – opaque minerals, glas – glass, id – iddingsite, rk – rock fragments. 22 DS, transmitted light, 1 polar

Ciemno i jasnobrązowe ziarna szkliva wulkanicznego, op – minerały kruszcowe, glas – szklivo wulkaniczne, id – iddyngsynt, rk – fragmenty skał. 22DS, światło przechodzące, 1 polaryzator.

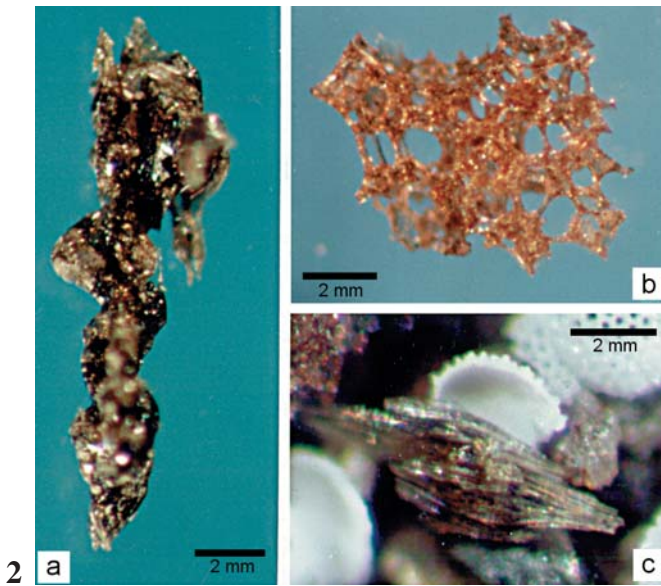
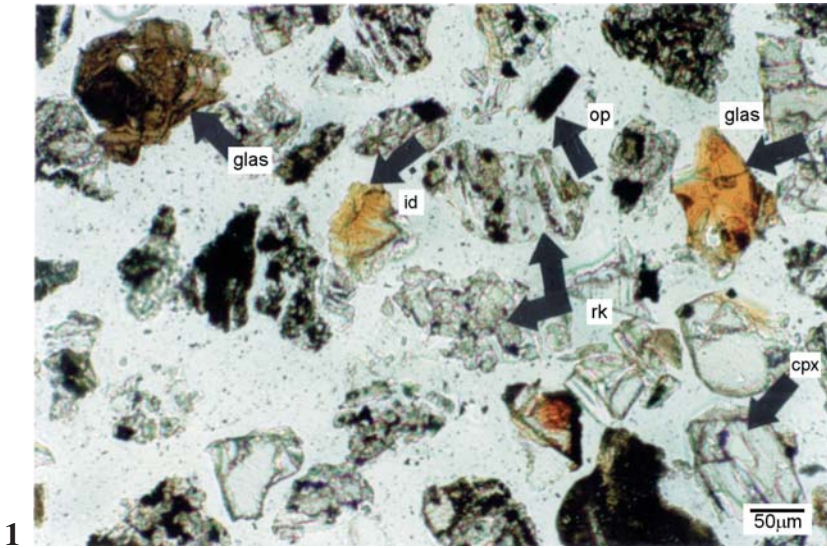
**2a.** Volcanic glass shard with many vesicles. 11 GKG, binocular microscope.

**b.** Volcanic glass shard in pipe shape. 11 GKG, binocular microscope. **c.** Spirally twisted volcanic glass shard. 11 GKG, binocular microscope.

**a.** Szklivo wulkaniczne z licznymi pęcherzykami. 11 GKG, lupa binokularna.

**b.** Szklivo wulkaniczne o kształcie rurkowym. 11 GKG, lupa binokularna

**c.** Skręcony spiralnie okruch szkliva wulkanicznego. 11 GKG, lupa binokularna.



in the form of sharp-edged, elongated fragments without vesicles or with bubbles shaped like narrow tubes (Pl. 2, Fig. 2b). Sometimes glass occurs in the form of spirally twisted shards (Pl. 2, Fig. 2c). In the sediments on the western and southern parts of the island massive shards of glass without bubbles were often found.

Two types of glass were identified in the population investigated microscopically: brown, described as dark and translucent, and light brown, described as bright (Pl. 2, Fig. 1). Altered glass, brown-golden, constitutes a separate group. The glass is generally strongly devitrified (Pl. 3, Fig. 1a). It often contains phenocrysts of pyroxenes and plagioclases (Pl. 3, Figs. 1b and 1c), particularly in the sample 11GKG.

Generally, there is 2–20 times more dark than bright glass (e.g. 35GKG 10–20, 18DS, 42SL460). In all sediments dark red glass shards have also been observed. The glass, different in colour under the microscope, has also a different chemical composition. With respect to the composition, two groups of glass shards were identified (Tab.1).

**Table 1.** Chemical composition of volcanic glass determined by electron microprobe method.

Skład chemiczny szkliwa wulkanicznego oznaczony przy użyciu mikros sondy elektronowej

	Dark glass (%)	Bright glass (%)
SiO <sub>2</sub>	48–52	62–65
Al <sub>2</sub> O <sub>3</sub>	11–15	15–17
FeO	11–14	7–13
CaO	9–12	~3
MgO	4–5	0–1
Na <sub>2</sub> O	3–4	–
K <sub>2</sub> O	1–2	~4
TiO <sub>2</sub>	–	~3

Bright glass, with the composition identical to that of dacite, has a higher content of SiO<sub>2</sub>, whereas dark glass, which can be called sideromelane, is characterized by a higher content of FeO, CaO, TiO<sub>2</sub> and smaller content of SiO<sub>2</sub>. Dark glass reveals signs of alteration (Pl. 3, Fig. 1b) and devitrification (Pl. 3, Figs. 1a and 1c), and consequently the sum of components expressed as percentage by weight can be considerably different than 100%. In 11 GKG and 35 GKG surface samples volcanic glass has a chemical composition similar to that of the glass from the oceanite series of *Piton de la Furnaise* (Fig. 10). In core samples 32SL, 42SL and 40SL at the depth of 360–460 cm the chemical composition is similar to that of the differentiated series glasses of *Piton des Neiges*.

## Other minerals

Other minerals of the heavy fraction include orthopyroxenes, amphiboles, biotite, apatite, staurolite and mineralised foraminifera (Fig. 9). Apart from orthopyroxenes the other components are very sporadic.

Biotite was found in the greatest numbers in box samples 8GKG, apatite and staurolite only in some samples from the 4SL profile. Mineralised remains of the microfossils, mainly foraminifera, mineralised with pyrite only, often occur in the sediments.

Amphiboles were found in significant quantities in the 42SL 330 sample, where they form characteristic green, strongly elongated, idiomorphic crystals. The optical features indicate minerals from the Ca-amphiboles group. On the basis of the chemical composition the minerals can be classified as magnesiohornblende. In other sediments of the 11GKG and 4SL profiles, amphiboles, yellowish-brownish, pleochroic, occur singly. In the 42SL sample, in addition to amphiboles, there are also rare orthopyroxenes.

## Opaque components

### Ore minerals

Among ore minerals the following were identified: magnetite, chromite and ilmenite. Spinels and ilmenite occur in great numbers as very fine particles (from several to a few score microns). Usually they form intergrowths with other minerals or they occur in basalt shards as phenocrysts. Isotropic magnetite, with the reflection ability of  $R < 20\%$ , and ilmenite, characterized by strong anisotropy, were determined microscopically. Ilmenite forms lamellae in magnetite. Chemical analyses have confirmed the presence of magnetite and Ti-magnetite, with up to 26% of  $\text{TiO}_2$ , and ilmenite (40SL 360, 42SL 330) with 49% of  $\text{TiO}_2$  and 44–49% of FeO. Pure magnetite containing 85% of FeO (32SL 460) is rare.

Framboidal pyrite was found in the 22DS and 4SL 20–25 samples, in the  $> 0.063$  fraction, particularly in the 0.25–0.5 mm range. Pyrite impregnates the remnants of foraminifera tests, and consequently mineralized bioclasts were also found in the heavy fraction of the sediment.

### Fe oxides

Fe oxides constitute a significant group separated from the heavy fraction. In smear slides they are clearly larger in size than other components (up to 2 mm).

These are oxides and hydroxides, with optical features of goethite or lepidol-

**Plate 3**

**1a.** Devitrified glass shards, sm – smectite, plag – plagioclase, glas – glass. 4 SL, BSE image. **b–c.** Alteration of glass shards through the palagonite stage to clay minerals, glas – glass. 4SL, BSE image.

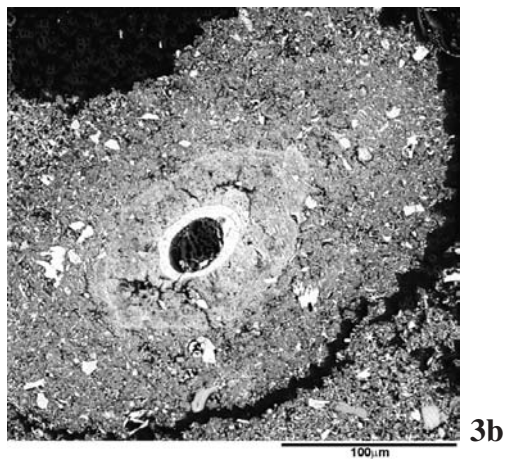
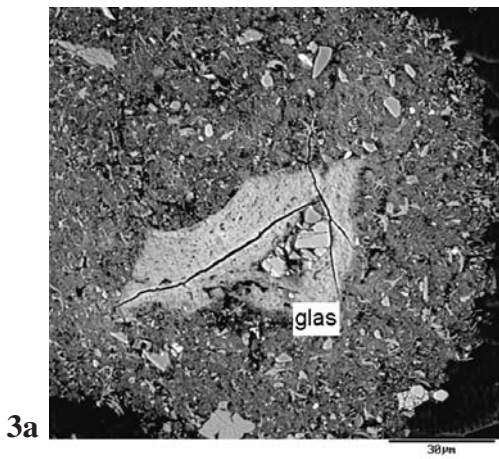
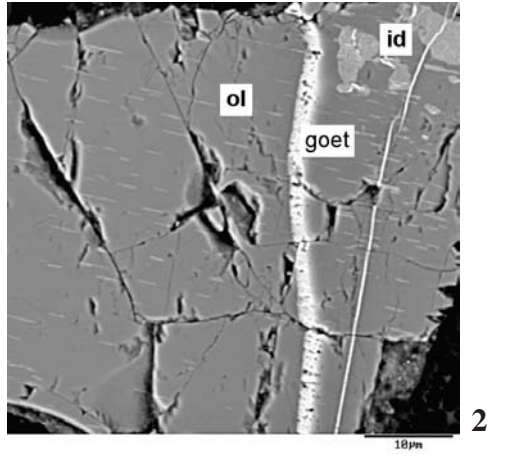
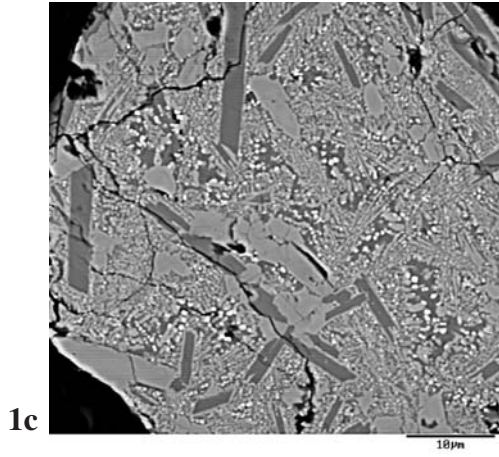
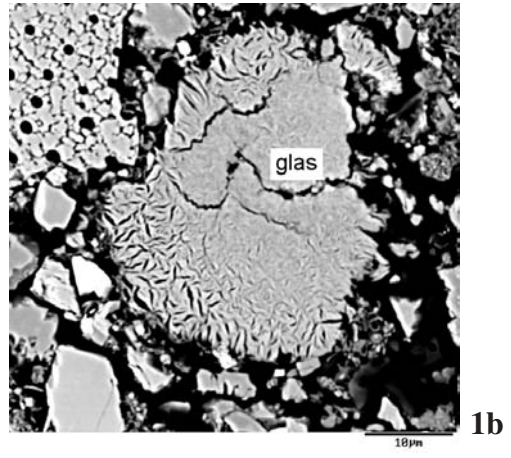
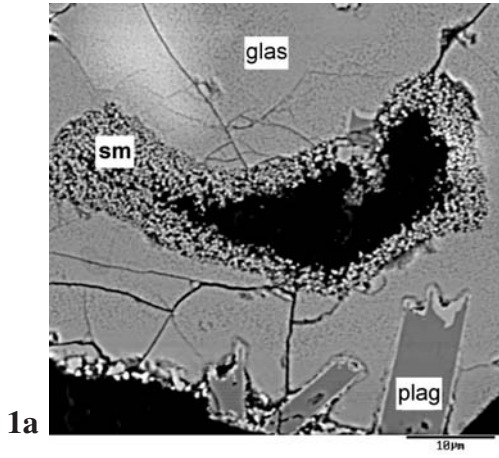
**a.** Zdewitryfikowane szkliwo wulkaniczne, sm – smektyt, plag – plagioklaz, glas – szkliwo wulkaniczne. 4SL, zdjęcie w elektronach wstecznie rozproszonych. **b–c.** Przeobrażenia szkliwa wulkanicznego przez stadium palagonitu do minerałów ilastych. 4SL, zdjęcie w elektronach wstecznie rozproszonych.

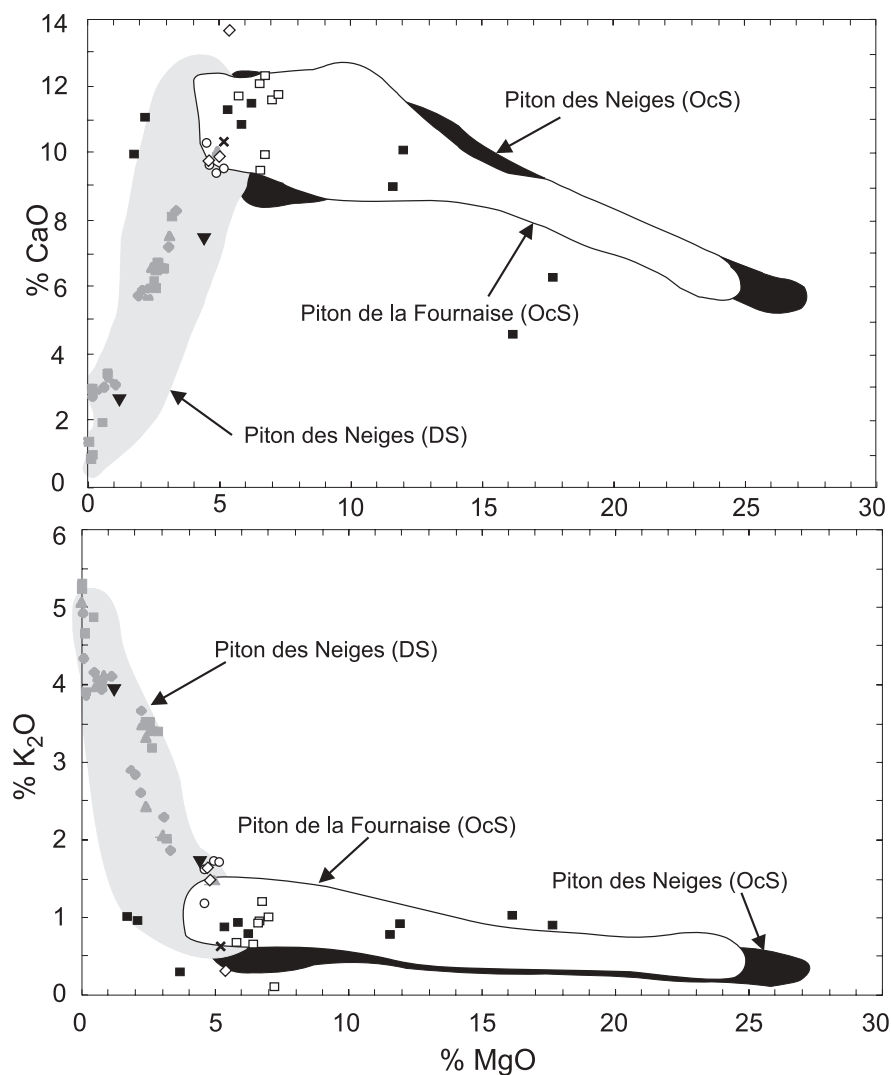
**2.** Fe-oxides (goethite and hematite) originated from olivine, ol – olivine, id – iddingsite, goet – goethite. 4 SL, BSE image.

Tlenki Fe (goezyt i hematyt) powstałe z oliwinu, ol – oliwin, id – idyngstyt, goet – goezyt. 4SL, zdjęcie w elektronach wstecznie rozproszonych.

**3a–b.** Microconcretions, glas – glass. 4 SL, BSE image.

Mikrokonkrecje, glas – szkliwo wulkaniczne. 4SL, zdjęcie w elektronach wstecznie rozproszonych.





Microprobe analyses of glass shards made in this work  
 Próbkę z których wykonano analizę szklę wulkanicznego mikrosondą elektronową.

- 11GKG
- ◇ 31 GKG
- 35 GKG
- 32 SL
- × 40 SL
- ▼ 42 SL

Samples analyzed by Fretzdorff (1997)  
 Próbkę analizowane przez Fretzdorff (1997).

- ◆ 17-662
- ▲ 17-656
- 17-666

**Fig. 10.** Chemical composition of volcanic glass in CaO and K<sub>2</sub>O versus MgO diagrams (all in % wt).

Skład chemiczny szklę wulkanicznego na diagramach CaO i K<sub>2</sub>O względem MgO (w % wag).

crocite. More detailed mineralogical and chemical determinations were very difficult and interpretation of results was uncertain due to the mixing of different phases or overlapping of the composition of the primary over the secondary mineral phase. In deep sea sediments, goethite, lepidocrocite, akaganeite, hematite and ferrihydrite are generally described (Burns & Burns 1979).

### Microconcretions

Microconcretions occur in the sediments from the 4SL profile and sporadically from the 22DS sections. Single forms were found in the heavy fraction (0.071–0.1 mm). Most often microconcretions are spherical, round or ellipsoidal in shape (Pl. 3, Figs. 2a and 2b), sometimes they occur as flattened reniform aggregates. They are present in all fractions of the 4SL profile, ranging in size from 4  $\mu\text{m}$  to 5 mm, usually 50–200  $\mu\text{m}$  (Pl. 3, Fig. 2a). In reflected light the forms under discussion do not have optical features typical of any known Mn mineral due to weak crystallinity, and the reflection ability is not much higher than in surrounding sediments. They are mainly composed of poorly crystalline Mn and Fe compounds (Fig. 11). They contain minimal quantities of Co, Ni and Cr.

Microconcretions have a brown colour under the microscope, in the reflected light a concentric structure can be observed in places. Mn and Fe content changes gradually from the highest value in the centre of the concretion to the minimal value in the surrounding sediment. In general, crystallization took place around the nuclei – bioclasts, crystals (pyroxene, plagioclase), lithoclasts or, which is most frequent, a volcanic glass shard (Pl. 3, Fig. 3a).

Other components of the heavy fraction, with a magnetite like composition, also occur in the concretion form. They form spherical aggregates, grey in the reflected light, isotropic, with a low reflection ability ( $R < 20\%$ ). Microprobe analyses have revealed iron as the main component of concretion. In the heavy fraction (0.071–0.1 mm) other components occur fairly sporadically; however, they were found in the sediments from different profiles (42SL, 4SL and 8GKG).

### Components of the pelitic fraction

Eighty samples were selected for mineralogical analyses. The two fractions under study, i.e.  $< 2\mu\text{m}$  and  $< 0.2\mu\text{m}$ , constitute less than 10% of the total sample mass.

In the samples, which have not been separated into fractions (analysed without any additional preparations), plagioclases, pyroxenes and calcite were found. These components are present in the samples in different proportions. Plagiocla-

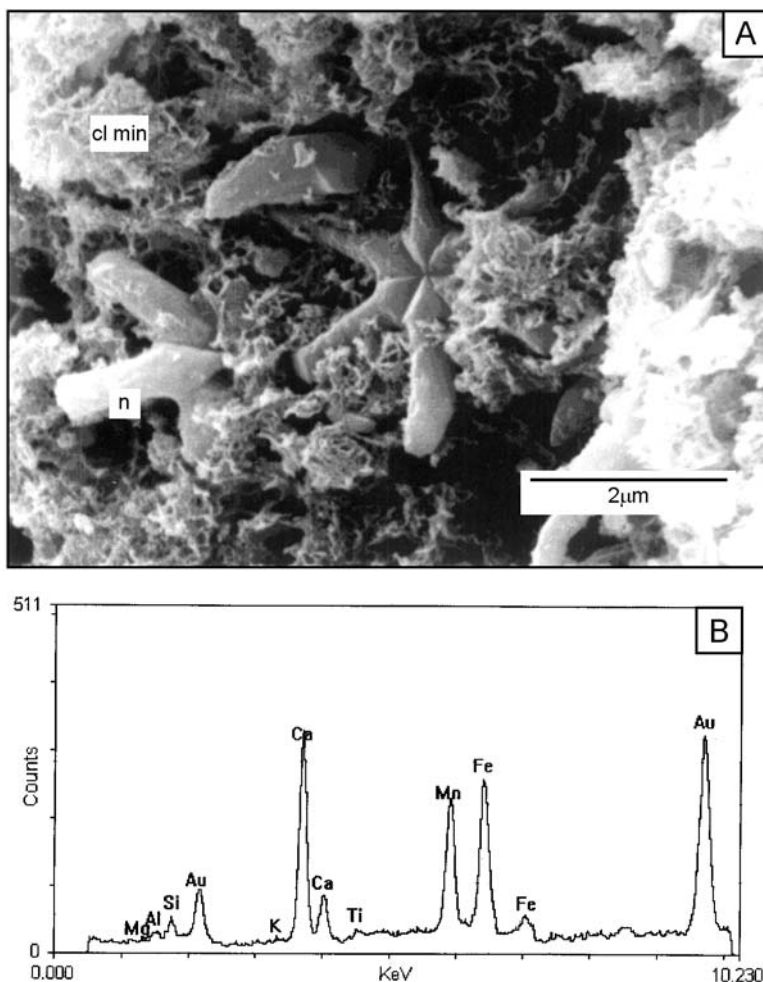


**Fig. 11.a.** SEM microphotograph of FeMn microconcretion, 4SL, cl – clay minerals, n – nanoplankton. **b.** Composition of microconcretions obtained by EDS method.

Obraz w mikroskopie skaningowym mikrokonkrecji Fe-Mn, 4SL, cl – minerały ilaste, n – nanoplankton. **b.** Skład mikrokonkrecji uzyskany w analizie EDS.

ses and pyroxenes are dominant in the sediments north (42SL, 47GKG, 46SL), west (11GKG) and south-west of the island (8GKG). In the western and south-western part (30SL, 36SL, 32 SL, 4SL), in addition to the phases mentioned above, calcite becomes an important component.

Zeolites were determined by the XRD method as phillipsite. Moreover, in the dry samples the 13–15 Å reflections were present, indicating clay phases from the smectite group. These phases were investigated in < 0.2 µm and < 2 µm fractions.

## Clay fraction

In the 42SL profile the largest quantity of clay minerals of all the profiles studied. In the  $< 2 \mu\text{m}$  fraction (random sample), in addition to plagioclases and pyroxenes, there are reflections indicating the presence of phillipsite and clay minerals from the smectite group.

In the  $< 0.2 \mu\text{m}$  fraction a high intensity reflection with  $d = 12.5\text{--}14.5 \text{ \AA}$  typical of minerals from the smectite group was observed. After glycolation the reflection moved to  $16.5\text{--}17 \text{ \AA}$  indicating the presence of a mineral of the smectite group (Figs. 12–16). An unquestionable determination of this phase requires registration of the reflection from the plane (060). However, when there are feldspars, pyroxenes and calcite in the samples, as a result of the coincidence of many reflections in the angular range of  $59\text{--}62^\circ 2\theta$ , it has not been possible to read the angle of the reflection from the plane (060). Smectite reflections are clear, symmetric after glycolation, which indicates a fairly homogeneous mineral. After heating the smectite reflection contracts to about  $10 \text{ \AA}$ .

In the 42SL section no changes of the mineralogical composition connected with the change of the depth are observed. Smectite occurred in all samples.

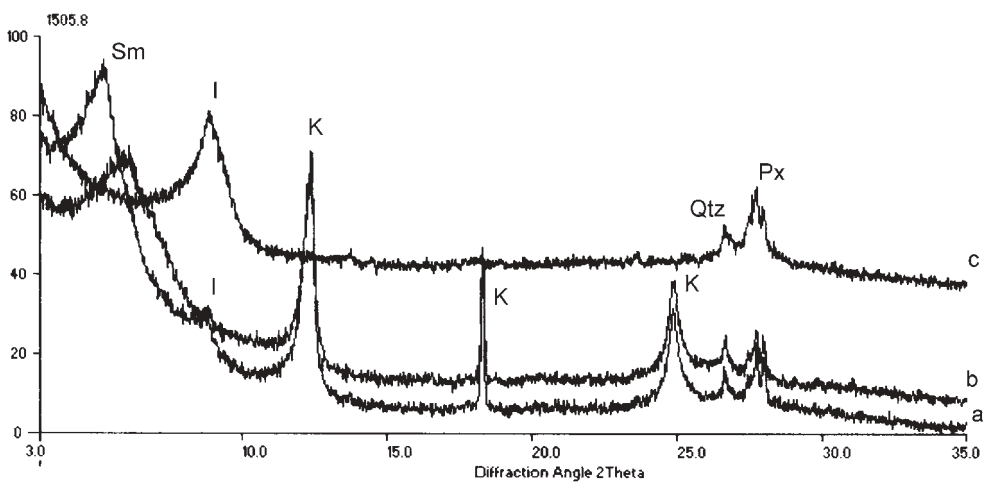
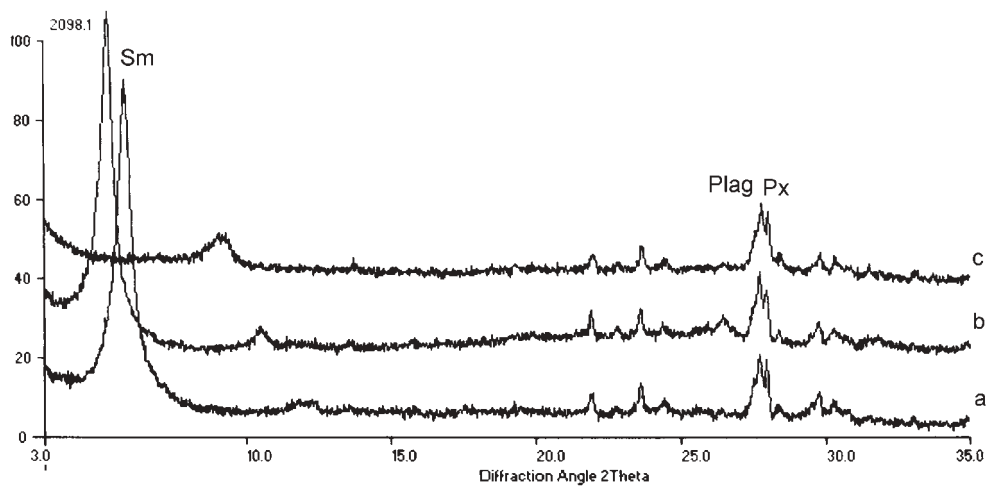
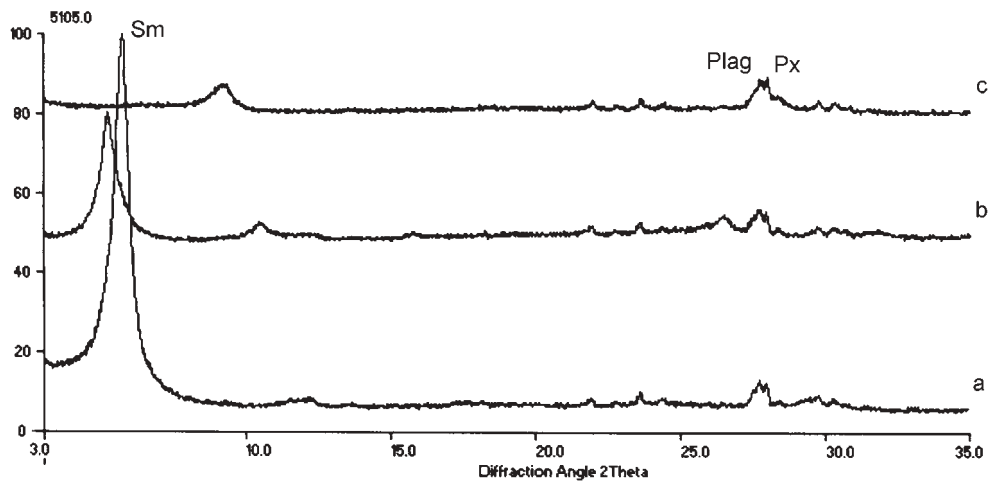
In the 30SL profile there are sediments with small quantities of clay minerals. In the  $< 2 \mu\text{m}$  fraction, down to the depth of 100 cm, mainly smectite ( $d 13.72\text{--}14.22 \text{ \AA}$ ) was detected. In this section also phillipsite was determined.

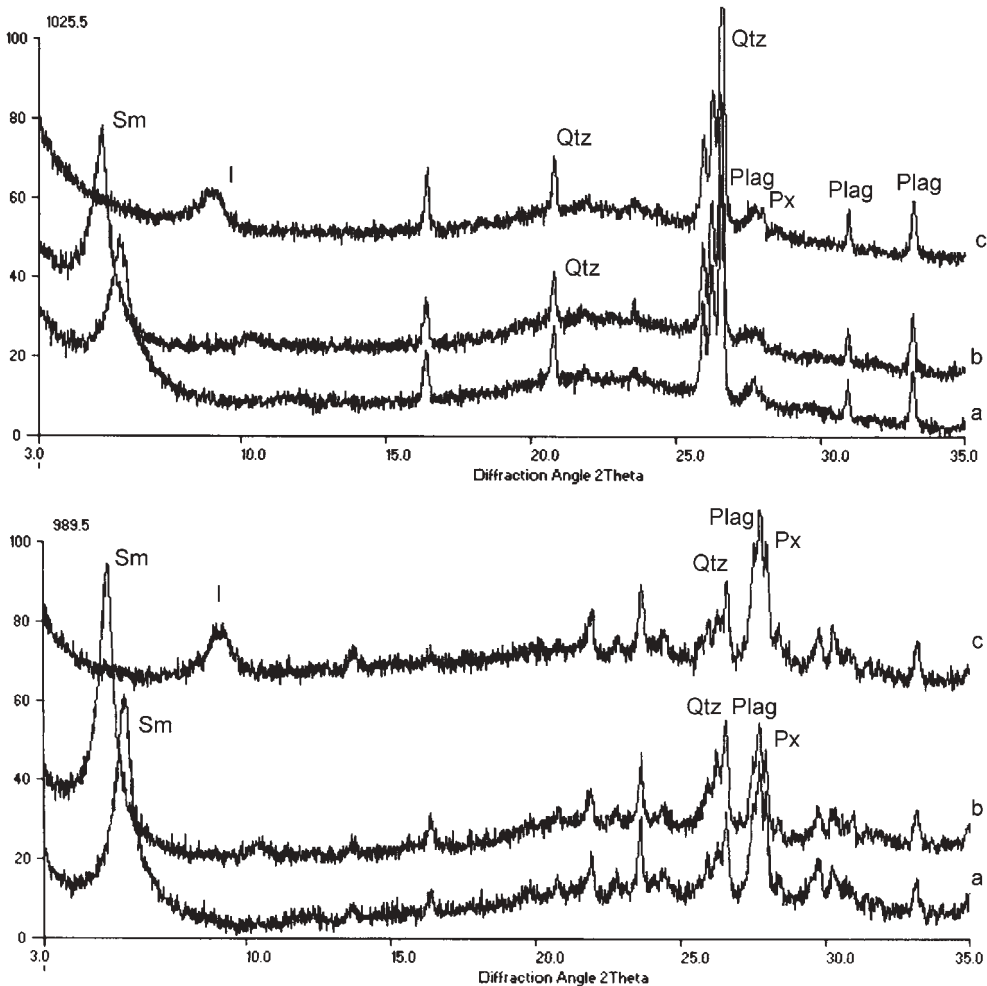
Profile 4SL, the southernmost sample point from the island, is characterized by the presence of kaolinite, identified from its 001 and 002 reflections ( $7.18 \text{ \AA}$  and  $3.58 \text{ \AA}$ ), which disappear after heating (Fig. 14).

In a few samples, in addition to smectite also white mica (illite) is present, which is manifested by the reflection of approximately  $10 \text{ \AA}$ . The reflection does not change its position after glycolation and increases after heating (Fig. 14).

In a few samples of the 32SL section amorphic substances have been identified. In general, quantities of clay minerals decrease and volcanogenic components, namely plagioclases and pyroxenes, increase with depth.

Apart from the sediments of the profiles discussed above, surface samples 22DS and 18DS and dredge samples (35GKG, 47GKG) were also analysed. They consist mainly of smectite and, depending on the position with respect to the island, there are additions of illite (35GKG). In the box samples 31GKG, kaolinite occur together with smectite in the top of the profile.





**Figs. 12–16.** XRD diffractograms of selected clay samples. a) oriented samples, b) glicolated samples c) heated in 550 °C. **Fig. 12.** 8GKG 0–5 cm, < 2  $\mu\text{m}$ . **Fig. 13.** 18DS, < 2  $\mu\text{m}$ . **Fig. 14.** 4SL 400–405 cm, < 2  $\mu\text{m}$ . **Fig. 15.** 42SL 200 cm, < 2  $\mu\text{m}$ . **Fig. 16.** 42SL 200 cm, < 0.2  $\mu\text{m}$ . Sm-smectite, I – Illite, K – kaolinite, Plag – plagioclase, Px – pyroxene, Qtz – quartz

Dyfraktogramy rentgenowskie wybranych próbek ilastych. a) próbki orientowane, b) próbki glikolowane, c) próbki wygrzewane w 550 °C. **Fig. 12.** 8GKG 0–5 cm, < 2  $\mu\text{m}$ . **Fig. 13.** 18DS, < 2  $\mu\text{m}$ . **Fig. 14.** 4SL 400–405 cm, < 2  $\mu\text{m}$ . **Fig. 15.** 42SL 200 cm, < 2  $\mu\text{m}$ . **Fig. 16.** 42SL 200 cm, < 0.2  $\mu\text{m}$ . Sm – smektyt, I – illit, K – kaolinit, Plag – plagioklaz, Px – piroksen, Qtz – kwarc.

## Discussion

The composition of the sediment light fraction is dominated by detrital components: lithoclasts and bioclasts, which originated as a result of pelagic

sedimentation in the ocean or hemipelagic sedimentation around the island (crystals, lithoclasts). Micrite and zeolites could have originated *in situ* or could have been transported over small distances.

The age of the sediments was determined on the basis of calcareous nannoplankton as Quaternary zones NN 21 (profile 42SL, bottom sediments: 22DS, 18DS, 31GKG), NN 20 and NN 21 (36SL, 32SL). The age complies with the chronostratigraphy made by Fretzdorff (1997). In 4SL profile there is a four-meter thick sequence of pelagic nannoplankton muds, originated in the Tertiary period which is confirmed by the discoasters: *D. brouweri* (NN 10–18), *D. pentaradiatus* (NN 10–17), *D. surculus* (NN 10–17), *D. petaliformis* (NN 4–5); the sequence is covered with Quaternary sediments. It is possible that these sediments constitute a turbidite sequence, as the sedimentological features typical of turbidites were observed (thickening of grains towards the bottom, traces of burrows at the top). The increase in the number of foraminifera in the 4SL profile also could be the result of turbidite sedimentation. Carbonate particles during this kind of sedimentation quickly pass through the zone of aggressive waters and in this way escape dissolution. In the deeper part of the 4SL core, at the depth of 80 cm below the ocean bottom, etched foraminifera tests can be observed. It was caused by the dissolution of carbonate skeletons at the lysocline, which in the western part of the Indian Ocean runs at the depth of 3700–3800 m (e.g. Seibold & Berger 1996).

Phillipsite occurs in all the sediments, however, its quantity depends on the distance from the island. Smallest quantities have been found in the 4SL profile, highest in 42SL one. As zeolites are unstable phases under the conditions of submarine weathering, they quickly transform into clay minerals, mainly smectites (Daymond *et al.* 1980; Kastner 1981). The occurrence of phillipsite as the product of basalt glass transformation in the sediment is fully justified (e.g. Rothwell 1987).

The composition of heavy fraction is dominated by volcanic material from the island. Non-volcanic components (e.g. staurolite) are rare; their presence is noticed in the profile most distant from the island. Samples, down to 30 cm below the ocean bottom, have mineral and chemical composition of the material from *Piton de la Furnaise*, whereas the samples from the deeper parts of the profiles – a composition typical of the material from *Piton des Neiges*. The only exception is the 32SL 320 sample, which is formed from the sediments bordering the oceanite series of *Piton des Neiges* and *Piton de la Furnaise*. The age of this layer of volcanic ashes was determined as 67 000 yrs (Fretzdorff 1997).

The composition of heavy fraction reflects immediate pyroclastic activity of the volcano or later mass flows transporting pyroclastic sediments to greater water depths. Most of the heavy mineral components in surface sediments located east and south of the island indicate a high sedimentation rate and the overwhelming influence of *Piton de la Furnaise* on the sedimentation.

The chemical composition of clinopyroxenes is typical of the basaltic rocks that form the *Piton des Neiges* and *Piton de la Furnaise*; its variability is a result

of geochemical evolution of magma (Tilley *et al.* 1971; Albarède & Tamagnan 1988; Fretzdorff 1997).

Magnesium pyroxenes originated earlier than the ferric ones and their chemical composition is typical for the parent magma of the Réunion type. Titanium augites, observed in samples 8GKG, 22DS (east and south of the island), are geochemically similar to the parent magma and, consequently, they could originate at almost the same time.

Primarily, olivines were phenocrysts in olivine basalts, of which the differentiated series of the *Piton des Neiges* and *Piton de la Furnaise* volcanoes are mainly formed. The rounding could be the result of melting of the crystal rims in volcanic processes, whereas its lack is the result of the short transport route. Paragenesis with spinels and kelyphite rims is connected with the initial stages of magma crystallization (e.g. Deer *et al.* 1997).

The massive fragments of glass without bubbles are transported to the sedimentation basin through dry surges and the volcanic ash fall, whereas shards with many bubbles are transported by wet surges and mass flows (Orton 1997).

On the basis of glass analysis it was shown that *Piton de la Furnaise* (presently active) has a greater influence on sedimentation of surface sediments; the deeper parts of the sediments are dominated with volcanic materials from *Piton des Neiges* (Fig. 12). This relation may indicate a greater force of the effusive activity of *Piton des Neiges* than that of the presently active volcano (Fretzdorff 1997). The sedimentation rate east of the island is twice higher than in the other areas, as a result of the sliding of enormous quantities of lava directly into the ocean and formation of huge debris flows (Ollier *et al.* 1998). Consequently, it is clear why volcanogenic sediments from this part of the ocean are geochemically similar to the lavas that form *Piton de la Furnaise*.

Ferric oxides observed in the heavy fraction, do not strongly cement the sediment but only form fragments, broken up due to the rewashing of the sediments and separation of the fraction. Forms of a similar type originate as a result of submarine weathering of basaltic rocks (Underwood *et al.* 1993; Baxter 1985) in the so-called basal parts of basalt covers in the spreading area. In the vicinity of Réunion weathering of pumice shards and fragments of basaltic rocks also results in the formation of clay minerals, which constitute a significant part of the studied sediments.

Iron minerals, i.e. goethite and hematite, occurring as clay-ferric clasts, could have originated as alteration of primary magnetite and ilmenite in the rocks. Hydrogenic phases – ferric-manganese concretions – originated *in situ* with the growth rate of a few mm/thousand years, determining the sedimentation rate in the 4SL profile. Manganese and iron compounds are dominant in the composition of microconcretions; they are accompanied by small quantities of Cu, Co and Ni.

The formation of pyrite is connected with early diagenesis under anaerobic conditions (Berner 1971), which could have existed locally at the ocean floor, where anaerobic bacteria can develop. Unstable forms of ferrous sulfides, grei-

gite ( $\text{Fe}_3\text{S}_4$ ) and mackinawite ( $\text{FeS}$ ), quickly change into pyrite, stable in a wide pH- and Eh-range of the environment. Supply of pyrite concretions from Réunion Island is hardly probable, since concretions occur only in the samples where ferric-manganese concretions were found.

Biotite was found in box samples 8GKG, apatite and staurolite only in some samples from the 4SL profile. As both profiles are the sample points most distant from the island (south-west and south-east), these components could have been transported by bottom currents from distant sources like Antarctica or Australia (Kolla *et al.* 1976). Spinels with a variable quantity of Cr originated in the early phases of crystallization due to magma differentiation and were frequently described as the product of basalt magma differentiation in the region of Réunion (Ludden 1978).

The sediments from 4SL profile are different than other sediments taken at a smaller distance from the island, not only with respect to the fossil assemblage but also with respect to the occurrence of manganese-ferric concretions (also quartz, staurolite, and apatite) and a greater degree of glass alteration. These sediments were formed under the conditions of pelagic sedimentation, and so the sedimentation rate facilitated the formation of concretions. Manganese could have originated from volcanic rocks or  $\text{Mn}^{+2}$  and  $\text{Fe}^{+2}$  ion carrying solutions, supplied from distant sources of alimentation by submarine currents.

The genesis of concretions can be related to the hydrodynamic conditions of water and the activity of aerobic and anaerobic bacteria, which destroy the organic matter, as is the case in the Baltic Sea (e.g. Glasby *et al.* 1997; Trokowitz 1998). The morphology of the smallest microconcretions observed and their homogenous chemical composition can confirm the role of bacteria in the formation of microconcretions. Microconcretions are the first stage of concretion formation. Saturation with Mn and Fe compounds occurs through the assimilation and cementation of different sediment components: crystals, nanofossils, zeolites, micrite and clay minerals. A gradual disappearance of Mn and Fe from the center to the edges of the concretion and diffused borders with the sediment indicate that they originated *in situ*. As is suggested by Piper & Blueford (1982), they should have been formed with the rate proportional to the sedimentation one.

Magnetite spherules can be of cosmic origin but they could have also originated as a result of volcanic processes (Morgan 1981; Bearman 1997). The origin of magnetite concretions connected with the hydrovolcanic activity (Iyer *et al.* 1997) and reactions of iron enriched lavas or emanation of hydrothermal solutions into the surrounding sediments of the Central Basin of the Indian Ocean is also suggested. The fairly rare occurrence of the spherical forms of magnetite in this area can be caused by hydrothermal activity (if the hydrovolcanic genesis is adopted) or the high sedimentation rate (in the case of the cosmic origin of concretions).

In 4SL, 32SL, 8GKG, 11 GKG and 22DS sections palagonite constitutes up to 50% of the total glass content. Both palagonite and bowlingite occur in the 4SL profile, which is probably connected with the long time that passed from sedimen-

tation to the present day, In box samples palagonite can be the result of the alteration of hot lava upon contact with sea water. These samples are within the reach of the youngest activity of *Piton de la Fournaise* (Philippot 1984; Fretzdorff 1997).

In the clay fraction smectite and kaolinite were determined by the XRD method. Smectite was described very often as an alteration product of basaltic rocks and volcanic glass and as a component of palagonite (Singer 1974; Schiffman & Southard 1996; Zevenberger *et al.* 1996).

In the western part of the Indian Ocean smectites constitute 70% of the clay fraction of bottom sediments (e.g. Kolla & Biscaye 1977): in the surface sediments in the direct vicinity of Réunion smectites comprise 100% of the clay fraction. Both Kolla *et al.* (1976) and Philippot (1984) suggest that both smectites and zeolites originated on the island as a result of hydrothermal processes. The analyses did not permit to differentiate among smectites that originated as a result of submarine weathering and that which originated as a result of precipitation from the oceanic water.

In all surface samples from the areas located close to the island (up to approximately 50 km), smectite is the dominant mineral of the clay fraction. In the 4SL profile, approximately 150 km away from the island, kaolinite, accompanied by smectite, is the dominant mineral of the clay fraction. Smectite present in the sediments of this profile results mainly from the alteration of basalt rocks that built Réunion. However, it is possible that some of smectites present in the sediments around the island were transported from the areas south of the island.

Kaolinite was found only in the 4SL profile, located south-west of the island. It is a mineral of detritic origin and can be transported over large distances. The southern part of the Indian Ocean is known for the presence of kaolinite (<10%, Kolla *et al.* 1976; Griffin *et al.* 1968; Goldberg & Griffin 1970). Kaolinite probably originates from weathered rocks of Western Africa or Australia (*ibid.*).

## Summary

1. Three sedimentary units could be identified in the bottom sediments of the Indian Ocean near Réunion Island based mainly on the ratios between volcanic and pelagic components, which reflect the distance from the island. The depth of the sea floor and the position with respect to Réunion determine the distribution of different sedimentary facies.

- Hemipelagic volcanogenic muds, most widely spread, occur at shallower water depths down to approximately 2000 m below water surface, in the direct vicinity of the island; they represent the sediments with highest sedimentation rate and consist mainly of volcanic material components.
- Pelagic foraminifera and nannoplankton oozes were found only in the 4SL profile, 150 km south-west of the island, at the depth of 3.5 km, where the influence of the material from the island is less visible; they consist mainly of pelagic bioclasts.

- Volcanic breccia sediments have been observed a few square score kilometres from the island, at waterdepths down to 2.5 km; they occur rarely in the ocean floor of the samples located north-east of the island and consist mainly of basaltic rocks (11GKG).

2. The age of the sediments was determined on the basis of carbonatic nannoplankton. In all the core sediments there are coccolites *Gephyrocapsa oceanica* (Quaternary zone NN 20) and *Emiliana huxleyi* (Quaternary zone NN 21). Discoasters, present in the 4SL profile (*Discoaster brouweri*, *Discoaster pentaradiatus*, *Discoaster surculus*, *Discoaster quinqueramus* (NN 10 to NN 18), indicate the Tertiary age. Singly occurred older forms (*Discoaster petaliformis*, NN 4–5) could be the result of redeposition.

3. The sediments analysed are mainly composed of lithoclasts (mainly basaltic rock fragments), crystals (plagioclases, pyroxenes, olivines), bioclasts (foraminifera, coccolites, discoasters) and clay phases, zeolites and carbonate mud, which cement the sediments.

4. The light fraction is composed of the detrital components: carbonate and siliceous bioclasts, feldspars, quartz, muscovite, carbonate mud, clay phases and authigenic components-zeolites and smectites.

5. In the heavy fraction basaltic rock fragments and clinopyroxenes are dominant; apart from them there are olivines, plagioclases with ore inclusions, volcanic glass, spinels and ilmenite. All the components have a volcanic genesis, so they are directly connected with Réunion. Other components of the heavy fraction, muscovite and staurolite occur sporadically in the core sample most distant from the island (4SL); they are the detrital components of the sediments.

6. The hydrogenic phase in the sediments is formed by microconcretions composed almost exclusively of manganese and iron oxides with some traces of Cu, Ni and Co, and by framboidal pyrite.

7. The samples have a fairly homogenous mineral composition of the pelitic fraction: the fraction  $< 2 \mu\text{m}$  contains smectite and zeolite; the fraction  $< 0.2 \mu\text{m}$  mostly smectite. Kaolinite occurs together with smectite in both fractions only in the southernmost core. Kaolinite is a detrital component, smectite is an authigenic mineral phase originating from the alteration of volcanic material.

8. The differences in the mineral composition of the sediments are the result of:

- the position of the sample point with respect to the island and its volcanic source-material (the farther from the island, the more components of pelagic sedimentation and the fewer volcanogenic components are found),
- depth from which the sediment was sampled: the quantity of clay minerals changes with depth; the composition and alteration of olivine and glass do not change with depth.

9. The influence of volcanism on sedimentation is following:

- nearly all the components of the heavy fraction come from Réunion Island,
- occurrences of dark red volcanic glass shards are the manifestations of the fumarole activity of the volcanoes on Réunion,

- it follows from the chemical composition of the glass shards that bottom surface sediments are derived from *Piton de la Fournaise*, the active volcano, whereas the components of the older sediments come from *Piton des Neiges*, the extinct volcano,
- the chemical and mineral composition of the main components of the heavy fraction helps to identify the areas which are under the influence of *Piton des Neiges* (west and north-west of the island) and *Piton de la Fournaise* (south, south-east and north-east of the island),
- the origin of authigenic phases (zeolites, palagonite, saponite) is connected with the alteration of the volcanogenic material at the early stages of diagenesis; it is possible that some of these phases were formed on the island and then were transported to the ocean.

10. Carbonate recrystallisation, mineralisation of foraminifera tests and the presence of framboidal pyrite are also manifestations of early diagenesis.

**Acknowledgements:** The authors gratefully acknowledge J. Biernacka, A. Muszyński and J. Środoń for their constructive comments on an earlier version of this paper. Prof. A. Muszyński, supervisor of the PhD thesis, is also acknowledged for critical reading and suggestions concerning dissertation. Special thanks to Jacek Czernikiewicz, who has been responsible for the graphic part of the paper, for technical support in preparation of the figures.

## References

- ALBARÉDE F., TAMAGNAN V., 1988: Modelling the recent geochemical evolution of the Piton de la Fournaise volcano, Réunion Island, 1931–1986. *Journal of Petrology*, **29**: 997–1030.
- BACMAN J., DUNCAN R.A., 1988: *Scientific Results of the Ocean Drilling Program*, **115**: 17–41.
- BASSINOT F.C., BEAUFORT L., VINCENT E., LABEYRIE L.D., ROSTEK F., MÜLLER P.J., QUIDELLEUR X., LANCELOT Y., 1994: Coarse fraction fluctuations in pelagic carbonate sediments from the tropical Indian Ocean: A 1500-kyr record of carbonate dissolution. *Paleoceanography*, **9**, 4: 579–600.
- BAXTER A.N., 1985: Major and trace elements variation in basalts from leg 115. *Scientific Results of the Ocean Drilling Program*, **115**: 19–21.
- BEARMAN G., 1997: Ocean chemistry and deep-sea sediments. The Open University, Pergamon, 134 pp.
- BERGER W.H., 1981: Oxygen and carbon isotopes in foraminifera: an introduction. *Palaogeography, Palaeoclimatology, Palaeoecology*, **33**: 3–7.
- BERNER R.A. 1971: Sedimentary pyrite formation. An update. *Geochimica Cosmochimica Acta*, **48**: 605–615.
- BURNS R.G., BURNS V.M., 1997, Marine Minerals. [In:] Burns R.G. (ed): *Reviews in Mineralogy*, **6**, 1–11.
- DAYMOND J., CORLISS J.B., COBLER R., MURATLI CH.M., CHOU CH., CONRAD R., 1980: Composition and origin of sediments recovered by deep drilling of sediment mounds, Galapagos spreading center. *Initial Reports of the Deep Sea Drilling Project*, **54**: 377–385.

- DEER W.A., HOWIE R.A., ZUSSMAN J., 1997: Rock-forming minerals. Single-Chain Silicates. The Geological Society, London, 667 pp.
- DENIEL C., KIEFFER G., LECOINTRE J., 1992: New  $^{230}\text{Th}$ - $^{238}\text{U}$  and  $^{14}\text{C}$  age determinations from Piton des Neiges volcano, Réunion – A revised chronology for the Differentiated Series. *Journal of Volcanology and Geothermal Research*, **51**: 253–267.
- DUCZMAL-CZERNIKIEWICZ A., 1999: Mineralogia osadów z rejonu wyspy Réunion (zachodni Ocean Indyjski). Unpublished PhD thesis, University of Poznań, 131 pp.
- DUNCAN R.A., BACKMAN J., PETERSON L., 1989: Réunion hot-spot activity through Tertiary time. Initial results from the Ocean Drilling Program. *Journal of Volcanology and Geothermal Research*, **36**: 193–198.
- DUNCAN R.A., 1990: The volcanic record of the Réunion Hot-spot. *Scientific Results of the Ocean Drilling Program*, **115**: 3–10.
- DUPLESSY J. C., BÉ A. W. H., BLANC P.L., 1981: Oxygen and carbon isotopic composition and biogeographic distribution of planktonic foraminifera in the Indian Ocean. *Palaeogeography, Palaeoclimatology, Palaeoecology*, **33**: 9–46.
- FISHER R.V., SCHMINKE H.-U., 1984: Pyroclastic Rocks. Springer, Berlin-Heidelberg, 472 pp.
- FRETZDORFF S., 1997: The Réunion Hotspot: History of explosive activity and geochemical evolution. *Berichte Reports*, Geologisch-Paläontologisches Institut Univ. Kiel, **81**, 98 pp.
- GILLOT P.-Y., LEFEVRE J.-C., NATIVEL P., 1994: Model for the structural evolution of the volcanoes of Réunion Island. *Earth and Planetary Science Letters*, **51**: 253–267.
- GILLOT P.-Y., NATIVEL P., 1982: K-Ar chronology of the ultimate activity of Piton des Neiges volcano, Réunion Island, Indian Ocean. *Journal of Volcanology and Geothermal Research*, **13**: 131–146.
- 1989: Eruptive history of the Piton de la Fournaise volcano, Réunion Island, Indian Ocean. *Journal of Volcanology and Geothermal Research*, **36**: 53–65.
- GLASBY G. P., EMELYANOV E. M., ZHAMOIDA V. A., BATURIN G. N., LEIPE T., BAHLO R., BONACKER P., 1997: Environments of formation of ferromanganese concretions in the Baltic Sea: a critical review. [In:] K. Nicholson *et al.* (Eds.): Manganese mineralization: geochemistry and mineralogy of terrestrial and marine deposits. *Geological Society of America Special Publ.*, **119**: 213–237.
- GOLDBERG E. D., GRIFFIN J. J., 1970: The sediments of the northern Indian Ocean. *Deep Sea Research*, **17**: 513–537.
- GRIFFIN J. J., WINDOM H., GOLDBERG E. D., 1968: The distribution of clay minerals in the World Ocean. *Deep Sea Research*, **15**: 433–459.
- IYER S.D., SHYAM PRADAS M., GUPTA S.M., CHARAN S.N., MUKHERJEE A.D., 1997: Hydrovolcanic activity in the Central Indian Ocean Basin. Does nature mimic laboratory experiments? *Journal of Volcanology and Geothermal Research*, **78**: 209–220.
- JACKSON M. L., 1975: The soil chemical analysis – Advanced course. 2<sup>nd</sup> edition. Published by the author, Madison, Wisconsin, 877 pp.
- KASTNER M., 1981: Autigenic silicates in deep-sea sediments formation and diagenesis. [In:] C. Emiliani (Ed): The Sea. The Oceanic Lithosphere. New York, 915–981.
- KOLLA V., BISCAYE P.E., 1973: Clay mineralogy and sedimentation in the eastern Indian Ocean. *Deep Sea Research*, **20**: 727–738.
- 1977: Distribution and origin of quartz in the sediments of the Indian Ocean. *Journal of Sedimentary Petrology*, **47**: 642–649.

- KOLLA V., HENDERSON L., BISCAYE P.E., 1976: Clay mineralogy and sedimentation in western Indian Ocean. *Deep Sea Research*, **23**: 949–961.
- LACROIX A., 1936: Le Volcan Actif de l'île de la Réunion et ses Produits. Paris, Gauthiers-Villars, 297 pp.
- LÉNAT J.-P., VINCENT P., BACHÉLERY P., 1989: The offshore continuation of an active basaltic volcano: Piton de la Fournaise (Réunion Island, Indian Ocean) structural and geomorphological interpretation of Sea Beam mapping. *Journal of Volcanology and Geothermal Research*, **36**: 1–36.
- LUDDEN J.N., 1978: Magmatic evolution of the basaltic shield volcanoes of Réunion Island. *Journal of Volcanology and Geothermal Research*, **4**: 171–198.
- MACDONALD G.A., KATSURA T., 1964. Chemical composition of Hawaiian Lavas. *Journal of Petrology*, **5**: 82–133.
- MCDUGALL I., 1971: The geochronology and evolution of the young volcanic island of Réunion, Indian Ocean. *Geochimica et Cosmochimica Acta*, **35**: 261–288.
- MOLNAR P., STOCK J., 1987: Relative motion of hotspots in the Pacific, Atlantic and Indian Oceans since Late Cretaceous time. *Nature*, **327**: 587–591.
- MOORE D.M., REYNOLDS R.C. JR., 1998: X-ray diffraction and the identification and analysis of clay minerals. Oxford University Press, New York, 332 pp.
- MORGAN, W.J., 1981: Hot-spot tracks and the opening of the Atlantic and Indian Oceans. [In:] C. Emiliani (Ed.): The Sea. The Oceanic Lithosphere, New York, 443–487.
- NERCESSIAN A., HIRN, A., LEPINE J.-C., SAPIN, M., 1996: Internal structure of Piton de la Fournaise volcano from seismic wave propagation and earthquake distribution. *Journal of Volcanology and Geothermal Research*, **70**: 123–143.
- OLLIER G., COCHONAT J.F., LÉNAT J.F., LABAZUY P., 1998: Deep-sea volcanoclastic sedimentary systems: an example from La Fournaise volcano, Réunion Island, Indian Ocean. *Sedimentology*, **45**: 293–330.
- ORTON G. J., 1997: Volcanic environments. [In:] H.G. Reading (Ed.): Sedimentary environments and facies. Blackwell Scientific Publications, Oxford, 485–567.
- PABLO-GÁLÁN L., CHÁVEZ-GARCÍA M., 1996: Diagenesis of Oligocene vitric tuffs to zeolites, Mexican Volcanic Belt. *Clays & Clay Minerals*, **44**: 324–338.
- PHILIPPOT F., 1984: La sédimentation volcanogène récente autour de l'île de la Réunion., Unpublished, Université de Paris-Sud, Orsay, 187 pp.
- PIPER D.Z., BLUEFORD J.R., 1982: Distribution, mineralogy, and texture of manganese nodules and their relation to sedimentation at DOMES Site A in the equatorial North Pacific. *Deep Sea Research*, **29**: 927–952.
- ROBINSON P.T., VON HERZEN R.P. 1989: College Station. *Scientific Results of the Ocean Drilling Program*, **118**: 3–235.
- ROCHER P., WESTERCAMP D., 1989: The Salazie Cirque ignimbrite (Piton des Neiges Volcano, Réunion Island): chronostratigraphy, description and significance of lithic fragments and eruptive mechanisms. *Journal of Volcanology and Geothermal Research*, **36**: 177–191.
- ROTHWELL R.G., 1987: The mineralogy of marine sediments. Elsevier Sc. Publ., Amsterdam, 234 pp.
- SAPIN, M., HIRN, A., LEPINE J.-C., NERCESSIAN A., 1996: Stress, failure and fluid flow deduced from earthquakes accompanying eruptions at Piton de la Fournaise volcano. *Journal of Volcanology and Geothermal Research*, **70**, 145–167.
- SHIFFMAN P., SOUTHARD R.J., 1996: Cation exchange capacity of layer silicates and pa-

- lagonitized glass in mafic volcanic rocks: a comparative study of bulk extraction and *in situ* techniques. *Clays & Clay Minerals*, **44**, 5: 624–634.
- SCHIFFMAN P., STAUDIGEL H., 1995: The smectite to chlorite transition in a fossil seamount hydrothermal system: the Basement Complex of La Palma, Canary Islands. *Journal of Metamorphic Geology*, **13**: 487–498.
- SEIBOLD E., BERGER W.H., 1996: The sea floor. An introduction to marine geology. Springer Verlag, Berlin, 356 pp.
- SINGER A., 1974: Mineralogy of palagonitic material from the Golan Heights, Israel. *Clays & Clay Minerals*, **22**, 3: 231–240.
- STOFFERS P., DEVEY C., ACKERMAND D., BERNER Z., CANTIN B., DURAND J., FRANKE-BRUCKMAIER B., FRETZDORFF S., GRAUPNER T., HAUG G., HEIKINIAN R., LABAZUY P., LORENC S., MÜHLHAN S., MÜHLHAN N., PARTERNE M., SCHMIDT M., STATTEGGER K., UHLIG S., WHITECHURCH H., 1994: Cruise report SO87: The Réunion Hotspot. *Berichte-Reports*, Geologische-Paläontologisches Institut Univ. Kiel, 65, 71 pp.
- TILLEY C.E., THOMPSON R.N., WADSWORTH W.J., UPTON B.G.J., 1971: Melting relations of some lavas of Réunion Island, Indian Ocean. *Mineralogical Magazine*, **38**: 344–352.
- TROKOWICZ D., 1998: Genesis of ferromanganese nodules in the Baltic Sea. *Prace PIG*, **163**: 1–62.
- TUCKER M.E., WRIGHT V.P., 1990: Carbonate sedimentology. Blackwell Sc. Publ., Oxford, 482 pp.
- UNDERWOOD M.B., PICKERING K., GIESKES J.M., KASTNER M., ORR R., 1993: Sediment geochemistry, clay mineralogy, and diagenesis: a synthesis of data from Leg 131, Nankai Trough. *Scientific Results of the Ocean Drilling Program*, **131**: 343–362.
- UPTON B.G.J., WADSWORTH W.J., 1965: Geology of Réunion Island, Indian Ocean. *Nature*, **207**: 151–154.
- 1966: The basalts of Réunion Island, Indian Ocean. *Bulletin of Volcanology*, **29**: 7–24.
- 1972a: Peridotite and Gabbroic Rocks Associated with the Shield-Forming Lavas of Réunion. *Contributions to Mineralogy & Petrology*, **35**: 139–158.
- 1972b: Aspects of magmatic evolution on Réunion Island. *Philosophical Transactions of the Royal Society of London, A.*, **271**: 105–130.
- VAN DER FLIER-KELLER E., 1991: Geochemistry and mineralogy of sediments, Atlantis II Fracture Zone, southwestern Indian Ocean. *Scientific Results of the Ocean Drilling Program*, **118**: 145–151.
- ZEVENBERGEN C., VAN REEUWIJK L.P., BRADLEY J.P., BLOEMEN P., COMANS R.N.J., 1996: Mechanism and conditions of clay formation during natural weathering of MSWI bottom ash. *Clays & Clay Minerals*, **44**, 4: 546–552.

## Charakterystyka osadów z rejonu wyspy Réunion (Zachodni Ocean Indyjski)

**Abstrakt:** Przedmiotem badań była charakterystyka osadów z rejonu wyspy Réunion na podstawie szczegółowej analizy petrograficznej i mineralogicznej. Osady z dna oceanu oraz rdzenie o długości do 560 cm (150 próbek) zostały zaklasyfikowane jako: hemipelagiczne muły wulkanogeniczne, pelagiczne muły węglanowe (nannoplanktonowe i otwornicowe) oraz wulkanogeniczna brekcja

bazaltowa. Brekcję bazaltową tworzą okruchy skał bazaltowych i szkliwa wulkanicznego. Muły wulkanogeniczne składają się głównie z fragmentów skał bazaltowych, minerałów pochodzenia wulkanicznego (plagioklazów, piroksenów i oliwinów), okruchów szkliwa wulkanicznego, zeolitów oraz minerałów ilastych. Ponadto występują w zmiennych ilościach bioklasty węglanowe i podrzędnie krzemionkowe. Muły pelagiczne są utworzone głównie z bioklastów węglanowych oraz mikrytu.

Skład mineralny oraz wzajemne relacje składników pelagicznych i wulkanogenicznych osadu są zdeterminowane głębokością i położeniem punktów badawczych względem wyspy. Osady z profilu położonego najbardziej na SE różnią się od innych położonych bliżej wyspy nie tylko zespołem skamieniałości, ale również występowaniem konkrecji (także kwarcu, staurolitu i apatyty) oraz większym stopniem przeobrażenia szkliwa wulkanicznego. Osady te powstawały w warunkach sedymentacji pelagicznej oraz powolnym tempem sedymentacji wyznaczonym przez formowanie się konkrecji.

Skład mineralny osadów zależy od odległości od wulkanicznej wyspy Réunion oraz od głębokości, z której osad był pobrany.

**Słowa kluczowe:** osady głębokomorskie, mineralogia, wyspa Réunion.

## Streszczenie

Wśród badanych utworów z dna Oceanu Indyjskiego w rejonie wyspy Réunion wyróżniono trzy grupy osadów, których rozmieszczenie jest zdeterminowane głębokością dna basenu oraz położeniem względem wyspy Réunion:

- muły hemipelagiczne z bioklastami, najszerzej rozprzestrzenione, występują na głębokości około 2000 m poniżej powierzchni wody w bezpośrednim sąsiedztwie wyspy; reprezentują osad o najszybszym tempie sedymentacji;

- muły pelagiczne otwornicowe i nanoplanktonowe stwierdzono jedynie w profilu 4SL oddalonym od wyspy o 150 km na południowy zachód, na głębokości 3,5 km, gdzie wpływ materiału z wyspy jest mniej widoczny;

- osady o charakterze brekcji wulkanicznej utworzyły się kilkadziesiąt kilometrów od wyspy na głębokościach do 2,5 km; występują podrzędnie w spągu profili usytuowanych na północ i północny-wschód od wyspy (42SL, 11GKG).

Wiek badanych osadów określono na podstawie nannoplanktonu wapiennego. We wszystkich osadach rdzeniowych występują kokkolity *Gephyrocapsa oceanica* (zona czwartorzędowa NN 20) oraz *Emiliana huxleyi* (zona czwartorzędowa NN 21). Występujące w profilu 4SL diskoastry, charakteryzujące się długimi zasięgami (*Discoaster brouweri*, *Discoaster petaliformis*, *Discoaster quinqueramus* – NN 4 do NN 18) wskazują na wiek trzeciorzędowy. Z uwagi na to, że w osadach występują diskoastry o różnych zasięgach, są one zapewne redeponowane, a redepozycja mogła zajść już w trzeciorzędzie (pliocenie).

Badane osady składają się głównie z litoklastów (głównie okruchów skał bazaltowych), krystaloklastów (plagioklaz, piroksen, oliwin), bioklastów (otwornice, kokkolity, diskoastry) oraz faz ilastych, zeolitów i mułu węglanowego, które stanowią spoiwo osadów. Frakcję lekką tworzą składniki detrytyczne: bioklasty

węglanowe i krzemionkowe, skalenie, kwarc muł węglanowy i fazy ilaste oraz składniki autigeniczne: zeolity i smektyty. We frakcji ciężkiej dominujący udział mają okruchy skał bazaltowych i klinopirokseny, ponadto występują oliwiny, plagioklasy z wrostkami kruszców, szkliwo wulkaniczne, spinele i ilmenit. Wszystkie wymienione składniki mają genezę wulkaniczną, związane więc są bezpośrednio z wyspą Réunion. Inne składniki frakcji ciężkiej, jak muskowitz i staurolit, występują sporadycznie w najbardziej oddalonym od wyspy profilu (4SL) i stanowią składniki detrytyczne osadów.

Fazę hydrogeniczną w omawianych osadach tworzą mikrokonkrecje złożone wyłącznie z tlenków manganu i żelaza, które występują w profilu 4SL i 22DS. W składzie chemicznym mikrokonkrecji stwierdzono śladowe ilości Cu, Ni i Co. Towarzyszy tym fazom występowanie framboidalnego pirytu.

Zbadane próbki odznaczają się dość jednorodnym składem mineralnym frakcji pelitowej: we frakcji  $< 2 \mu\text{m}$  występują smektyty, zeolity i miejscami domieszki miki typu illitu, we frakcji  $< 0.2 \mu\text{m}$  głównie smektyty. Kaolinit i smektyty występują w obu wydzielonych frakcjach w profilu najbardziej na południe oddalonym od wyspy (4SL). Kaolinit i illit są składnikami detrytycznymi osadu, smektyty – składnikami autigenicznymi.

Różnice w składzie mineralnym osadów wynikają ze zróżnicowanego położenia punktów badawczych względem wyspy (im dalej od wyspy, tym więcej składników sedymentacji pelagicznej a mniej wulkanogenicznych), a także głębokości pobrania osadu (z głębokością zmienia się ilość minerałów ilastych, nie zmienia się ich skład ani intensywność przeobrażeń oliwinów i szkliwa).

Wpływ wulkanizmu na sedymentację osadów był następujący:

- niemal wszystkie składniki frakcji ciężkiej pochodzą z wyspy Réunion;
- ze składu chemicznego okruchów szkliwa wynika, że osady powierzchniowe pochodzą z aktywnego wulkanu *Piton de la Furnaise*, natomiast składniki starszych osadów pochodzą z wygasłego *Piton des Neiges*;
- skład chemiczny i mineralny głównych składników frakcji ciężkiej pozwala wskazać obszary, które pozostają pod wpływem aktywności wulkanu *Piton des Neiges* (na zachód i północny-zachód od wyspy) i *Piton de la Furnaise* (na południe, południowy wschód i północny wschód od wyspy);
- powstanie minerałów autigenicznych (zeolity, palagonit, smektyt) jest związane z przeobrażeniem materiału wulkanogenicznego we wczesnych etapach diagenety; nie można wykluczyć, że część tych faz utworzyła się na wyspie, a następnie została przetransportowana do zbiornika;
- ponadto z działalnością piroklastyczną wulkanów tworzących wyspę można wiązać powstanie warstw popiołów wulkanicznych w osadach rdzeniowych (Fretzdorff 1997).

Przejawami wczesnej diagenety są w omawianych osadach procesy: rekrytalizacji węglanów, okruszczenia otwornic oraz powstanie framboidalnego pirytu.

**Appendix 1.** Location of sediment stations of the recovered samples (after Stoffers *et al.* 1994).

Położenie punktów badawczych, z których pobrano osady (wg Stoffersa i in. 1994).

No.	Marks of samples		Investigated area	Geographical coordinates	Water depth (m)	Length of core
1	17 635-1	4 SL 6	SW of Réunion	22° 47,95' S 54° 56,24' E	3684	5,52 m
2	17 639-1	8 GKG	SE of Réunion	22° 00,41' S 56° 20,02' E	4167	0,40 m
3	17 641-1	11 GKG	WNW of Réunion	21° 00,11' S 56° 25,35' E	3862	0,35 m
4		18 DS	S of Réunion	21° 39,58' S 55° 38,42' E to 21° 39,37' S 55° 38,69' E	2265  2155	
5		22 DS	S of Réunion	21° 34,68' S 55° 28,13' E to 21° 34,21' S 55° 28,86' E	2239  1928	
6	17 655-1	29 GKG	SW of Réunion	21° 36,80' S 55° 16,81' E	2321	0,42 m
	17 655-2	30 SLS 4	SW of Réunion	21° 36,80' S 55° 16,80' E	2321	4,40 m
7	17 656-1	31 GKG	SW of Réunion	21° 54,20' S 55° 18,20' E	3806	0,45 m
8	17 656-2	32 SLS 6	SW of Réunion	21° 54,20' S 55° 18,20' E	3807	4,66 m
9	17 659-1	35 GKG	W of Réunion	21° 00,20' S 54° 40,85' E	3545	0,40 m
10	17 659-2	36 SL	W of Réunion	21° 00,10' S 54° 40,85' E	3545	1,90 m
11	17 662-1	39 GKG	N of Réunion	20° 30,25' S 55° 51,22' E	3094	0,40 m
12	17 662-2	40 SLS 10	N of Réunion	20° 30,20' S 55° 51,20' E	3095	6,40 m
13	17 663-1	41 GKG	N of Réunion	20° 40,35' S 55° 30,85' E	1918	0,33 m
14	17 663-2	42 SLS 10	N of Réunion	20° 40,36' S 55° 30,85' E	1923	5,55 m
15	17 666-2	46 SLS 10	NW of Réunion	20° 36,50' S 55° 00,80' E	3290	6,30 m

**Appendix 2.** Selected chemical analyses of clinopyroxenes. (EMP) mikro-probe analyses.

Wybrane analizy chemiczne klinopiroksenów. Analizy wykonane mikrosondą elektronową.

Sample	31 GKG30-40	35 GKG 20-30	4 SL 40-50			
	clinopyroxene	clinopyroxene	clinopyroxene	clinopyroxene	clinopyroxene	clinopyroxene
No	1	2	3	4	5	6
SiO <sub>2</sub>	50.47	47.34	49.37	50.14	50.82	50.56
TiO <sub>2</sub>	1.94	2.33	1.63	1.53	1.34	1.16
Al <sub>2</sub> O <sub>3</sub>	4.69	5.47	3.31	3.14	3.18	3.91
Cr <sub>2</sub> O <sub>3</sub>	–	–	0.08	0.02	0.12	1.18
FeO	7.65	7.62	10.55	9.86	7.69	5.64
MnO	0.13	0.00	0.32	0.23	0.04	0.23
NiO	0.02	0.00	–	–	–	–
MgO	13.66	13.50	14.03	14.37	15.73	15.59
CaO	22.09	22.39	19.91	20.28	20.36	20.61
Na <sub>2</sub> O	0.43	1.32	0.32	0.42	0.28	0.32
K <sub>2</sub> O	0.00	0.00	0.01	0.01	0.01	0.02
Total	101.08	99.97	99.53	99.99	99.57	99.23
Si	1.8565	1.7796	1.8654	1.8786	1.8894	1.8756
Ti	0.0536	0.0657	0.0462	0.0432	0.0372	0.0324
Al	0.2034	0.2423	0.1476	0.1386	0.1392	0.1710
Cr	–	–	0.0024	0.0006	0.0036	0.0348
Fe	0.2353	0.2394	0.3336	0.3090	0.2394	0.1746
Mn	0.0039	0.0000	0.0102	0.0072	0.0012	0.0072
Ni	0.0004	0.0000	–	–	–	–
Mg	0.7488	0.7565	0.7902	0.8022	0.8718	0.8622
Ca	0.8705	0.9020	0.8064	0.8136	0.8106	0.8190
Na	0.0308	0.0959	0.0234	0.0306	0.0204	0.0234
K	0.0000	0.0000	0.0006	0.0006	0.0006	0.0006
Total	4.0032	4.0812	4.0260	4.0242	4.0134	4.0008
Si IV	1.8565	1.7796	1.8654	1.8786	1.8894	1.8756
Al IV	0.1435	0.2204	0.1346	0.1214	0.1106	0.1244
Fe + <sup>3</sup> IV	0.0000	0.0000	0.0000	0.0000	0.0000	0.0000
T	2.0000	2.0000	2.0000	2.0000	2.0000	2.0000
Al VI	0.0599	0.0218	0.0130	0.0172	0.0286	0.0466
Ti	0.0536	0.0657	0.0462	0.0432	0.0372	0.0324
Fe <sup>+2</sup>	0.2353	0.2394	0.3336	0.3090	0.2394	0.1746
Mn	0.0039	0.0000	0.0102	0.0072	0.0012	0.0072
Mg	0.7488	0.7565	0.7902	0.8022	0.8718	0.8622
Ca	0.8705	0.9020	0.8064	0.8136	0.8106	0.8190
Na	0.0308	0.0959	0.0234	0.0306	0.0204	0.0234
K	0.0000	0.0000	0.0006	0.0006	0.0006	0.0006
M 1, M 2	2.0028	2.0812	2.0236	2.0236	2.0098	1.9660
<i>Wo</i>	46.94	47.52	41.78	42.28	42.20	44.14
<i>En</i>	40.38	39.86	40.94	41.68	45.36	46.44
<i>Fs</i>	12.69	12.62	17.28	16.04	12.45	9.42

**Appendix 3.** Selected chemical analyses of plagioclases. (EMP) microprobe analyses.

Wybrane analizy chemiczne plagioklazów. Analizy wykonane mikrosondą elektronową.

Sample	40 SL 258	42 SL 135			42 SL 490		
	plagioclase	plagioclase	plagioclase	plagioclase	plagioclase	plagioclase	plagioclase
No	1	2	3	4	5	6	7
SiO <sub>2</sub>	55.41	58.67	58.47	55.34	59.72	51.99	50.67
TiO <sub>2</sub>	0.24	0.16	0.20	0.28	0.28	0.09	0.12
Al <sub>2</sub> O <sub>3</sub>	27.67	25.53	25.85	27.09	24.87	29.86	30.67
Cr <sub>2</sub> O <sub>3</sub>	0.00	0.00	0.00	0.00	0.01	0.00	0.00
FeO	0.00	0.61	0.65	1.19	1.10	0.81	0.88
MnO	0.00	0.03	0.04	0.07	0.01	0.01	0.07
NiO	–	–	–	–	–	–	–
MgO	0.17	0.03	0.04	0.28	0.09	0.14	0.09
CaO	11.18	7.56	7.75	10.11	7.54	13.15	13.93
Na <sub>2</sub> O	4.66	6.79	6.72	5.57	6.32	3.98	3.35
K <sub>2</sub> O	0.60	0.57	0.55	0.49	0.90	0.10	0.24
Total	99.92	99.95	100.26	100.42	100.86	100.13	100.02
Si	2.5008	2.6320	2.6168	2.5008	2.6584	2.3656	2.3168
Ti	0.0080	0.0056	0.0064	0.0096	0.0096	0.0032	0.0040
Al	1.4720	1.3496	1.3640	1.4432	1.3048	1.6016	1.6528
Cr	0.0000	0.0000	0.0000	0.0000	0.0008	0.0000	0.0000
Fe	0.0000	0.0224	0.0248	0.0448	0.0408	0.0312	0.0336
Mn	0.0000	0.0008	0.0016	0.0024	0.0008	0.0008	0.0032
Ni	–	–	–	–	–	–	–
Mg	0.0120	0.0016	0.0024	0.0184	0.0064	0.0096	0.0056
Ca	0.5408	0.3632	0.3712	0.4896	0.3592	0.6408	0.6824
Na	0.4080	0.5904	0.5832	0.4880	0.5456	0.3504	0.2968
K	0.0344	0.0328	0.0312	0.0288	0.0512	0.0056	0.0136
Total	4.9760	4.9984	5.0016	5.0256	4.9776	5.0088	5.0088
<i>Or</i>	<i>1.14</i>	<i>1.22</i>	<i>1.17</i>	<i>0.96</i>	<i>1.98</i>	<i>0.18</i>	<i>0.42</i>
<i>Ab</i>	<i>27.07</i>	<i>44.27</i>	<i>43.46</i>	<i>32.93</i>	<i>42.29</i>	<i>21.44</i>	<i>17.80</i>
<i>An</i>	<i>71.80</i>	<i>54.51</i>	<i>55.37</i>	<i>66.11</i>	<i>55.72</i>	<i>78.38</i>	<i>81.78</i>

**Appendix 4.** Selected chemical analyses of olivines. (EMP) microprobe analyses.  
Wybrane analizy chemiczne oliwinów. Analizy wykonane mikrosondą elektro-  
nową.

Sample	35 GKG > 40	4 SL 40–50			30 SL 90	40 SL 148	42 SL bottom
	olivine	olivine	olivine	olivine	olivine	olivine	olivine
No	1	2	3	4	5	6	7
SiO <sub>2</sub>	39.54	41.80	41.04	39.32	36.68	39.21	41.97
TiO <sub>2</sub>	0.02	0.06	0.00	0.06	0.06	0.75	0.00
Al <sub>2</sub> O <sub>3</sub>	0.05	0.47	0.02	0.03	0.00	0.55	0.09
Cr <sub>2</sub> O <sub>3</sub>	–	0.00	0.04	0.08	–	–	–
FeO	19.21	4.06	9.45	16.38	30.36	30.04	11.60
MnO	0.28	0.18	0.34	0.23	0.58	0.85	0.16
NiO	0.20	–	–	–	–	0.08	0.21
MgO	40.46	52.93	49.02	43.55	31.68	27.30	46.66
CaO	0.24	0.53	0.09	0.36	0.34	0.79	0.29
Na <sub>2</sub> O	0.00	0.03	0.03	0.00	0.08	0.35	0.04
K <sub>2</sub> O	0.00	0.02	0.00	0.00	0.00	0.12	0.00
Total	100.00	100.08	100.02	100.01	99.78	100.04	101.02
Si	1.0125	0.9976	1.0040	0.9952	0.9980	1.0570	1.0236
Ti	0.0003	0.0012	0.0000	0.0012	0.0012	0.0151	0.0000
Al	0.0013	0.0132	0.0004	0.0008	0.0000	0.0176	0.0026
Cr	–	0.0000	0.0008	0.0016	–	–	–
Fe	0.4114	0.0812	0.1932	0.3468	0.6908	0.6773	0.2366
Mn	0.0061	0.0036	0.0072	0.0048	0.0132	0.0194	0.0032
Ni	0.0040	–	–	–	–	0.0017	0.0041
Mg	1.5440	1.8832	1.7872	1.6428	1.2848	1.0968	1.6960
Ca	0.0065	0.0136	0.0024	0.0096	0.0100	0.0227	0.0074
Na	0.0000	0.0016	0.0012	0.0000	0.0040	0.0182	0.0021
K	0.0000	0.0004	0.0000	0.0000	0.0000	0.0041	0.0000
Total	2.9861	2.9956	2.9964	3.0028	3.0020	2.9299	2.9756
<i>Fo</i>	78.96	95.87	90.24	82.57	65.03	61.83	87.76
<i>Fa</i>	21.04	4.13	9.76	17.43	34.97	38.17	12.24